Eur. Phys. J. E (2015) **38**: 13
DOI 10.1140/epje/i2015-15013-8

THE EUROPEAN PHYSICAL JOURNAL E

Regular Article

Thinning and thickening of free-standing smectic films revisited

Elena S. Pikina[1,2,a], Boris I. Ostrovskii[3,2], and Wim H. de Jeu[4]

[1] Oil and Gas Research Institute, Russian Academy of Sciences, Gubkin str. 3, 119333 Moscow, Russia
[2] Landau Institute for Theoretical Physics of the RAS, 142432 Chernogolovka, Russia
[3] Institute of Crystallography, Russian Academy of Sciences, Leninsky pr. 59, 119333 Moscow, Russia
[4] DWI - Leibniz Institute for Interactive Materials, RWTH Aachen University, D-52056 Aachen, Germany

Received 14 October 2014 and Received in final form 22 January 2015
Published online: 9 March 2015 – © EDP Sciences / Società Italiana di Fisica / Springer-Verlag 2015

Abstract. We present a theoretical explanation of the remarkable thickness instabilities that occur in free-standing smectic films (FSSF) upon changing the external conditions: i) upon heating the film above the bulk smectic disordering temperature, generally the film does not rupture but instead shows successive layer-by-layer thinning transitions; ii) thickening of FSSF, which occurs within the thermal range of the smectic phase upon local heating. All observations reported so far can be explained on the basis of the Landau-de Gennes theory of the smectic state in combination with nucleation theory. In overheated smectic films (thinning) or locally heated FSSF (thickening) an additional normal tensile force appears due to a change of the mean density of the film. In the case of an overheated FSSF the free energy has oscillatory character, and upon heating the balance of tensile and elastic forces breaks down spontaneously. This leads to thinning of the film, which proceeds via thermal nucleation and growing of dislocation loops in the middle plane of the film. The expression for the envelope of the points of thinning as well as estimates of the dynamics of growth of dislocation loops, are in good agreement with experiments. Local heating of a FSSF within the smectic temperature range induces thermal expansion, which shifts the system to a metastable state. This favors nucleation and growth of dislocation loops of excess smectic layers in the middle plane of the film. The activation energy of such dislocation loops attains values below the threshold energy and decreases upon further heating. This leads to local film thickening by many tens of layers. Realization of this scenario depends crucially on the energy dissipated locally in the film. Estimates of the thickness of the growing "island" in the film and of the velocity of the dislocation loop growth are in reasonable agreement with experiments.

1 Introduction

The smectic-A phase (Sm-A) consists of elongated molecules arranged in stacks of liquid layers in which the long molecular axes are, on average, parallel to the layer normal. When stretched on a frame, these materials, due to their layered structure, can form free-standing smectic films (FSSF) [1] in which the smectic layers align parallel to the two air-film interfaces. Hence in a FSSF a thin layer of smectic liquid is bounded by two free surfaces. The film is attached to its frame via a meniscus, which serves as a reservoir with which the film can exchange matter (see fig. 1). Apart from the edges such films can be considered as substrate-free.

There is a vast literature on FSSF; see, for example, [2–8] for an overview of early work up to about 1996. More recent reviews are given in [9–11]. This paper presents a theoretical study of the thermal stability of FSSF, which remains one of the challenging and unresolved issues in the field of smectic films. In spite of extensive experimental and theoretical work, there are open questions regarding the origin of thinning transitions in the overheated FSSF as well as of thickening of free smectic films that can occur within the thermal range of the smectic phase.

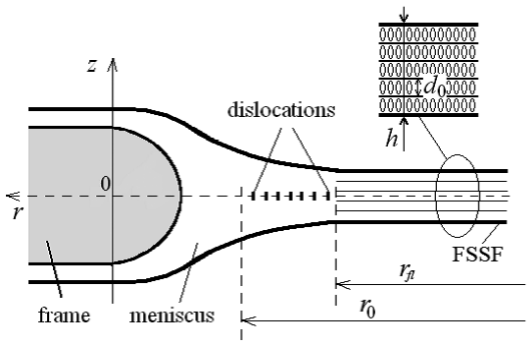

Fig. 1. Sketch of the free-standing smectic film stretched on a frame.

[a] e-mail: elena@ogri.ru

The theoretical precursor to describe the above effects is the de Gennes theory of the pre-smectic ordering [12] (see also [13]). The notion "pre-smectic liquid" refers to a nematic liquid crystal above the phase transition to the Sm-A phase, where effects of short-range smectic order are well developed. In the original paper [12] the pre-smectic liquid is confined between two parallel solid surfaces. In the case of FSSF the smectic liquid is confined between two free surfaces and connected at the periphery with the surrounding volume reservoir-meniscus. As a result the thickness of the film, h, turns up to be the free thermodynamic parameter. Gorodetskii *et al.* [14] were the first to use this approach to explain thermal instabilities in FSSF under the assumption of an external compressive force applied to the free surfaces of the film. If overheated above the bulk smectic A-nematic transition temperature ($T_{\rm NA}$) or smectic A-isotropic temperature ($T_{\rm IA}$), a long-wavelength thickness instability develops because the external compressive and elastic forces can no longer be balanced for a fixed number of smectic layers. The stability can be restored by spontaneous thinning of the film to a thickness corresponding to a smaller number of smectic layers [14]. In general, the process involves a series of such thinning transitions [6–8]. However, the concept of an external compressive force is rather ambiguous, and actually the film appears to be stretched along the layer normal. As a consequence the thermodynamic conditions for a series of thinning transitions are not well determined. Below we provide a fully consistent description of the thinning transitions in overheated films.

Thickening is quite an unusual effect in FSSF. The first clear observation goes back to a paper of de Jeu *et al.* [15], in which thickening of a FSSF was detected over the footprint of a synchrotron X-ray beam incident below the critical angle of total reflection. The authors attributed the thickening to local heating at one side of the film due to absorption by the evanescent wave. In the illuminated area the tension of the FSSF is supposed to be not supported anymore by an elastic stress of smectic layers, which triggers off a chain reaction of material flow. However, the precise mechanism of the thickening, which involves generation of edge-dislocation loops, remained unclear. Also, the role of heat conduction, as well as of the dynamics of the process, were not considered.

In this paper we propose a theoretical explanation for the observed thickening effect. Generally speaking, nonuniform heating of the medium causes additional stress. This effect should be incorporated in the variation of the free energy of the system. Under these conditions the average density of liquid crystal differs from the undisturbed state [16]. This leads to additional contributions to the free-energy density of the system, the most important one arising from local thermal expansion. We show that at relatively large heating (but not too large to avoid any transition to the nematic or isotropic state) nucleation and growth of dislocation loops of the excess smectic layer becomes energetically favorable. The necessary material for growth of the additional layer is provided by the meniscus.

In the following we first discuss experimentally the instabilities in FSSF, including methods of preparation and observation. The main focus of the remaining sections is a theoretical description of thermal instabilities in FSSF. In sect. 3 some basic theoretical aspects are summarized. In sects. 4 and 5, respectively, thinning transitions and the thickening effect are discussed theoretically. Section 6 is devoted to dynamics of dislocation loops growth. Finally sect. 7 gives a concluding discussion. Theoretical details of the discussion are included in the appendices.

2 Overview of experimental results

Free-standing smectic films can be drawn manually by wetting the edges of an opening in a glass or metal holder with smectic material and then moving a spreader across the hole [17]. Alternatively a frame with a variable area can be used [3, 4, 10]. After preparation, such a film consists of regions of different thickness, from which it equilibrates to a uniform situation. Usually the thinnest region grows at the expense of the thicker ones and the final state depends on the way the film has been created.

Since the early work of Pieranski *et al.* [3], the (meta) stability of FSSF has been discussed by several authors [18–21]. Geminard *et al.* [18] studied the meniscus surrounding a needle in a FSSF by observing the fringes in monochromatic light. The results show that the meniscus consists of a collection of steps due to edge dislocations repelled from the free surfaces (see fig. 1). In fact, the meniscus consists of a thick part with a large density of dislocations, and a thinner part adjacent to the film in which dislocations remain elementary [19, 20]. The latter part can be fitted by a circular profile which for thick films matches tangentially the free surface of the film [19, 20]. For films less than about 50 layers this behavior changes and an apparent "contact" angle appears.

Thickness variations in a FSSF usually proceed via nucleation of edge-dislocation loops [18, 19, 21]. Application of a local heat pulse, which brings the film locally to a transition to either the nematic or the isotropic phase, can generate such an elementary loop. Subsequently, the size of the loop increases, provided it exceeds a certain critical radius. This behavior is related to the phenomenon of thinning transitions. The FSSF can be heated above the bulk smectic disordering temperature without immediately rupturing, and instead undergo successive layer-by-layer thinning transitions as the temperature is increased [5, 22, 23]. Thinning transitions have been first observed in fluorinated mesogens at the smectic A-isotropic transition and subsequently also at the Sm A-nematic phase transition of certain mesogens [7, 20, 24, 25]. The important experimental observable is the variation of the layer-thinning transition temperature $T_c(N)$ with N, the number of layers in the film. $T_c(N)$ can be well fitted by the power-law relation $N \propto \tau^{-\varsigma}$, where $\tau = [T_c(N) - T_c]/T_c$, $\varsigma \simeq 0.70 \pm 0.10$, and T_c is close to the bulk transition temperature.

At present there is no theoretical consensus about the mechanism by which thinning occurs. An initial believe was that thinning takes place when the smectic layer structure in the middle of a film vanishes [26–29]. In an alternative theory [14], supported by experimental studies [30,31],

layer thinning occurs by spontaneous nucleation of dislocation loops prior to the melting of the layer structure in the film interior. Actually these two approaches are related, since a sufficient reduction in the degree of smectic order is required to generate an elementary dislocation loop. Furthermore, it is not clear whether the experimental results on thinning at (first-order) smectic-isotropic transitions and (second- or first-order) smectic-nematic transitions all can be treated within the same framework.

The first observation of thickening in FSSF was made in paper [15], using a synchrotron X-ray beam incident below the critical angle of total reflection. The experiments were made on 3 to 80 layer films of the liquid crystal compound 4O.8. The thickness was found to grow at (and only at) the footprint of the beam, reaching in a few tens of minutes hundreds of layers ($\simeq 0.5\,\mu$m). The thick island thus formed is not connected to the meniscus and the surrounding area keeps the original thickness (see fig. 1 in [15]). There is no difference between thick and thin films, apart from the fact that the thickening is much faster in thin films. In particular, a four-layer film was investigated in some detail: the thickness was found to increase within minutes to many tens of layers. The necessary material for the thicker part is provided by the meniscus and can only flow via the smectic layers of the original film. For incoming angles exceeding the critical angle of total reflection, the thickening does not occur and the film remains stable. This is a crucial observation, suggesting strongly that dissipation of energy by the evanescent wave in a thin surface layer might be responsible for the thickening. The effect is quite general and has been observed in FSSF of several compounds. The process is reversible, unlike radiation damage observed in many polymer and liquid films under high-flux synchrotron irradiation. After the illumination is switched off, the footprint "island" slowly breaks up. Finally, with time the various thick parts disappear in the meniscus and the film returns to its initial state.

Another observation of the film thickening corresponds to somewhat exotic conditions [32]. Photosensitive FSSF of smectic C material were studied under white light illumination. Smectic C differs from Sm A: the long molecular axes are, on average, tilted with respect to the layer normal. For appropriate light and thermal conditions, a layer-by-layer thickening process could be detected in the illuminated film area. The new aspect is that thickening occurs under light illumination instead of a temperature change. However, the liquid crystalline molecules contained azobenzene fragments, which are known to undergo a conformational transition from the *trans* to *cis* state on absorbing light of an appropriate wavelength. The *cis* isomers are strongly bent and no longer contribute to the nematic or smectic ordering. In fact, they act as impurities and destabilize the smectic order. In bulk liquid crystals, this leads to a shift of the phase transitions towards low temperatures. In that sense illumination by light plays a similar role as a temperature increase and effectively reduces the smectic order. From that point of view the two experiments, with X-rays and light, are quite similar.

3 Theoretical aspects of the stability of FSSF

3.1 Basic equations

A bulk smectic A phase with mean density ρ_0 is characterized by a density modulation along the z axis perpendicular to the smectic layers:

$$\rho(z) = \rho_0 + \sqrt{2}\varrho_1 \cos[q_0 z + \phi], \tag{1}$$

where ϱ_1 is the amplitude of the first harmonic of the smectic density wave, $q_0 = 2\pi/d_0$ is a wave number of the smectic layering with periodicity d_0, $\phi = q_0 u$ is an arbitrary phase associated with the layer displacement u from the equilibrium position. Note that ϱ_1 is the amplitude of the complex order parameter characterizing the smectic ordering, while ϕ is its phase.

In the following we consider a flat FSSF with a meniscus in which the total amount of material does not change. The excess of the total energy $F_{\rm tot}$ of the system has the form:

$$F_{\rm tot} = 2\,\pi\,\gamma\,{r_{fl}}^2 + \Delta F + \int_0^{r_0} 2\,\pi\,r\,{\rm d}r \left[\frac{\rho_0\,g\,h^2}{2} + 2\left\{\frac{\Phi}{\delta h_{st}^3}\left(\frac{{\rm d}h/2}{{\rm d}r}\right)^3 + E_d\,\frac{1}{\delta h_{st}}\frac{{\rm d}h/2}{{\rm d}r}\right\}\right], \tag{2}$$

where γ is the interface tension, $r = r_{fl}$ is the point matching of the meniscus with the planar part of the film (see fig. 1), r_0 is the characteristic radius of the meniscus, which is measured from the center of the circular opening in the frame, ΔF is the excess of the free energy of FSSF due to its finite thickness, h is the current thickness of the film, and g is the gravitational acceleration. The other two terms under the integral are related to dislocations in the system, E_d is the line energy of the elementary edge dislocation, Φ is the amplitude of entropic repulsion between dislocations and δh_{st} is height of the transitional edge profiles at the film surface (details in appendix A).

To solve the problems related with the thickness instabilities of FSSF it is important to find all contributions to $F_{\rm tot}$, and then determine the temperature dependence of the equilibrium film thickness taking the external influences on the system (see below) into account.

3.2 Thermodynamics of FSSF under external action

First we derive the free-energy contributions corresponding to deviation of the density of the system from its initial average equilibrium value $\rho_0 \to \rho_0 + \delta\rho$ under influence of some external action. From conservation of the total mass, we can write $\delta\rho(\rho_0)^{-1} = -\delta V V_0^{-1}$, which is valid up to first-order corrections ($\delta\rho$ is the variation of the average density and δV the corresponding change of the initial volume V_0). Let ϖ be the free energy per unit mass (see, for example [33]). Then $\rho_0\varpi$ is the free-energy density (per unit volume) of the condensed medium. Quite generally, the variation of the free energy of the system due to

changes of the density can be written as $d\varpi = p\rho_0^{-2} d\rho_0$, where p is the pressure of the system. Expanding $\rho_0\varpi$ into a series over $\delta\rho$, up to second-order terms, we arrive at

$$\big((\rho_0+\delta\rho)\varpi\big) \approx \rho_0\varpi_0+\delta\rho\frac{\partial(\rho_0\varpi)}{\partial\rho_0}+\frac{(\delta\rho)^2}{2}\frac{\partial^2(\rho_0\varpi)}{\partial\rho_0^2}\,. \quad (3)$$

Using the thermodynamic relation for the variation of the free energy influenced by the density changes, $\delta\rho$, we can write $(\partial(\rho_0\varpi)/\partial\rho_0)_S = \varpi + p\rho_0^{-1}$, $(\partial^2(\rho_0\varpi)/\partial\rho_0^2)_S = c^2\rho_0^{-1}$, where $c \approx 1.5\cdot 10^3\,\mathrm{m\,s^{-1}}$ is the speed of the "first" sound [16], and eq. (3) now reads

$$\big((\rho_0+\delta\rho)\varpi\big) \approx (\rho_0+\delta\rho)\varpi_0 + \frac{p}{\rho_0}\delta\rho + \frac{c^2}{\rho_0}\frac{(\delta\rho)^2}{2}\,. \quad (4)$$

Keeping this in mind, the excess of the free energy of FSSF, ΔF (see eq. (2)), as a function of a number of thermodynamic parameters and of a temperature variation as an external field can be presented in the following form ($V \approx V_0 + \delta V$):

$$\begin{aligned}\Delta F = &-p_{Sm}^{(L)}V_0(1-\vartheta) + \frac{A}{2}\,\vartheta^2\,V_0\\ &+ A\,\kappa\,\Delta T\,V_0\,\vartheta - \int_0^{r_0} 2\,\pi\,r\,\mathrm{d}r\int_{-h/2}^{h/2}\mathrm{d}z\,C\,\vartheta(\nabla_z u)\\ &+ \int_0^{r_0} 2\,\pi\,r\,\mathrm{d}r f_{Sm}[h], \end{aligned} \quad (5)$$

where $\Delta T = T - T_0$ is a temperature change of the system, and

$$\vartheta = \frac{\delta\rho}{\rho_0[T_0]}\,, \quad (6)$$

where $\delta\rho = \rho_0 - \rho_0[T_0]$ is a variation of the mean density with temperature. In the following we will use the function $f[\vartheta, h]$, which determines the density per unit area of the free-energy ΔF (eq. (5)) and can be expressed via $\Delta F = \int_0^{r_0} 2\pi r\,\mathrm{d}r f[\vartheta, h]$. The $f[\vartheta, h]$ function can be written as

$$\begin{aligned} f[\vartheta,h] = &-p_{Sm}^{(L)}h(1-\vartheta) + \frac{A}{2}\,\vartheta^2\,h\\ &+ A\,\kappa\,\Delta T\,\vartheta\,h - C\,\vartheta\,\frac{\Delta\phi}{q_0} + f_{Sm}[h], \end{aligned} \quad (7)$$

where $\Delta\phi = q_0(u[h/2] - u[-h/2])$.

The first term in eq. (7) is the "fluid" part of the free energy, not related to smectic order. It determines the liquid-like contribution to the pressure of the film $p_{Sm}^{(L)}$ at $T = T_0$.

The second term in eq. (7) is quadratic in ϑ (*i.e.* proportional to $\delta\rho^2$), and is commonly used in the theory of propagation of the acoustic waves (see for example [33], p. 306) and also in the theory of elasticity of solids, $A = \rho_0 c^2 \approx 2.2\cdot 10^9\,\mathrm{J\,m^{-3}}$ [16].

The third term in eq. (7) is proportional to the variation of temperature ΔT. It is typical for the elastic theory of solids relating strain and temperature change. In our case ΔT plays a role of external field with respect to ϑ (see for example [34], p. 28), and the coefficient κ is the volume thermal expansion modulus. The value of κ can be deduced from the dilatometer measurements of the derivative $\mathrm{d}V/\mathrm{d}T$ at atmospheric pressure. For the liquid crystal 4O.8 in smectic phase it is of the order of $\sim 10^{-3}\,\mathrm{K^{-1}}$ [35,36].

The next term in eq. (7) refers specifically to smectics and takes any external action on the system into account. In the present case there is the gradient of displacement of the smectic layers, $(\nabla_z u)$, as well as the relative density variation, ϑ, that should be considered as independent variables (see [16] pp. 338, 508).

Finally, the last term in eq. (7) is the excess of Landau-de Gennes free-energy density of the FSSF [16,20]

$$\begin{aligned} f_{Sm}[h] = \int_{-h/2}^{h/2}\mathrm{d}z\Big\{ &\frac{\alpha_0\,\tau}{2}\,\varrho_1^2 + \frac{\beta}{4}\,\varrho_1^4\\ &+ \frac{\alpha_0\,\xi_{0\|}^2}{2}(\nabla_z\varrho_1)^2 + \frac{\alpha_0\,q_0^2\,\xi_{0\|}^2}{2}\,\varrho_1^2(\nabla_z u)^2\Big\}, \end{aligned} \quad (8)$$

where α_0 and β are positive phenomenological constants, and $\tau = (T - T_{\mathrm{NA}})/T_{\mathrm{NA}}$. The terms with ∇_z account for spatial variations of the smectic order parameter, where $\xi_{\|0}$ represents the bare value of the longitudinal smectic correlation length ($\xi = \xi_{\|0}|\tau|^{-1/2}$). The above equation is quite general and has been systematically used for theoretical description of smectic films in different confinement, for example films in the cells [37,38] and in porous medium [39].

In relation to the third and fourth terms of eqs. (5) and (7) we note that static distortions of the smectic layers are usually considered for constant average density. This condition not true anymore in case of external action that changes the mean density of the medium (see [16] pp. 338, 508). For example, heating a film produces uniform volume dilation and nonuniform displacement of the smectic layers due to confinement by the boundaries. In this case in addition to layer displacements, $u(z)$, we have to introduce one more independent variable ϑ, determining the temperature variation of the relative mean density of the smectic film, eq. (6).

According to eq. (7), the free energy of the system is a functional of a relative density ϑ and an equilibrium thickness h, which serve as free variables and depend on temperature variation ΔT as an external parameter. Thus, in order to find equilibrium values of the mean density and the film thickness we consider the variation of eq. (7) over ϑ and h, and derive the equilibrium conditions. Herewith, the variation of eq. (7) over ϑ in the absence of external tangential stresses gives the pressure in the system multiplied by h, while variation over h determines the interaction force per unit surface between the free boundaries of the film.

Upon applying any external action on the FSSF, the first reaction is adjustment of the mean density ρ_0, and not of smectic layer displacements $u[z]$. This is because the conventional speed of sound c_1 is much larger than the speed of the "second sound" c_2, which corresponds to a modulation of u: $c_2 \sim u/t$. The density variation

is described by terms in eq. (7) that depend on ϑ. This, in turn, leads to additional interaction between the free surfaces of the film, which is compensated by the elastic response of the smectic layers.

Note that the concept of pressure is in smectic films not as simple as in ordinary liquids. In lamellar systems the pressure is generally not equal with that of the surrounding medium [40], even in the case of a plane interface. For example, when the external pressure is raised to a high level, or, otherwise, the container with the film is evacuated to low values [15], the system fails to compensate for these variations by changing the mean density. In this case the pressure difference can be written as

$$\Delta p = p_{Sm}^{(L)} - p_{\rm air}, \tag{9}$$

and the system reacts via dilation of the smectic layers. As a result, equilibrium of forces acting on the free surfaces of the FSSF necessary involves the smectic elasticity. However, in certain cases the pressure in the smectic can be equated to that of the surrounding gas ($\Delta p = 0$). This assumption is valid for relatively small changes of the external pressure, when the equation of state of the smectic is close to that of an ordinary liquid (see [34], p. 242). For example, a FSSF is usually made either at atmospheric pressure or in a chamber at a slightly lower pressure [5,6,8]. Then the variation of pressure is compensated by changes of the mean density. This approach will be used in the next section in the description of thinning instabilities in overheated FSSF.

4 Thinning transitions in overheated FSSF ($T > T_{NA}$)

4.1 De Gennes model

As discussed earlier, the de Gennes model [12] of the presmectic liquid was the first to show implicitly of metastability of overheated smectic films confined between two parallel solid surfaces. The surfaces induce smectic ordering at $T > T_{\rm NA}$. The generalization of the de Gennes model to different types of boundary conditions was given in ref. [41]. The application to overheated FSSF and an analysis of the range of their meta(stability) have been first made by Gorodetskii, Pikina and Podnek [14]. Various aspects related to thinning transitions have been discussed by a number of authors [20,28,30,31]. In the following we attempt to build a consistent theory of the thinning transitions in overheated FSSF.

We recall eq. (1) for the complex order parameter of smectics, in which ϱ_1 is the amplitude of the density wave and $\phi[z] = q_0 u[z]$ its phase. Hence minimization of the free energy of the FSSF is carried out with respect to both ϱ_1 and $\phi[z]$ (or $u[z]$). It is important that ϱ_1 changes below smectic-nematic transition according to a power law: $\varrho_1 \propto ((T - T_{\rm NA})/T_{\rm NA})^{\chi}$, where χ is the critical index. This leads to nontrivial behaviour of both ϱ_1 and $u[z]$ in the vicinity of the phase transition, thus determining the meta(stable) character of the system. At the same time the change of the mean equilibrium density ρ_0 associated with the temperature variation is monotonic and noncritical.

Following de Gennes, only quadratic terms are essential in the excess Landau-de Gennes free energy of the film (per unit area) above the temperature of the bulk NA-transition $T_{\rm NA}$ [12,14,41] (compare with eq. (8)):

$$f_{Sm}^{(T>T_{\rm NA})}[h] = \frac{\alpha_0 \tau}{2} \int_{-h/2}^{+h/2} {\rm d}z \Big\{ \varrho_1^2 + \xi^2 \big((\nabla_z \varrho_1)^2 + q_0^2 \varrho_1^2 (\nabla_z u)^2 \big) \Big\}. \tag{10}$$

Let the free surfaces bounding the FSSF of thickness h be located at $z = \pm h/2$ (see fig. 1). Now the amplitude of the order parameter describing the overheated smectic film $\varrho_1[z]$ and layer displacement $u[z]$ vary nonuniformly between the film interfaces.

As usual, we assume

$$h \gg \xi \gg q_0^{-1}, \tag{11}$$

the condition of applicability of the long-wave approximation in eq. (10).

Following de Gennes [12], it is natural to assume the positions of the maxima of the smectic density wave to be fixed on the free surfaces of the film. Taking into account that the functional, eq. (10), is invariant to a change of the sign of ϱ_1, this means

$$q_0 (h + 2u[h/2]) = 2\pi N, \tag{12}$$

where N is the number of smectic layers, the integer nearest to h/d_0. It is useful to introduce also the phase difference $[\phi]_N$ describing the deviation of the film thickness h from the unperturbed values $h_N = N d_0$. The relations given above lead to $[\phi]_N = q_0 (h - N d_0)$.

Minimization of eq. (10) with respect to $\varrho_1[z]$ and $u[z]$ gives the system of Euler differential equations, that can be solved taking the boundary conditions (12) into account. Note that the coupling term of ρ_0 and $u[z]$ does not contribute to the Euler equation due its linearity in the gradient of $u[z]$. After integration of eq. (10) with fixed surface value of the squared amplitude $(\varrho_1[\pm h/2])^2 \equiv \varrho_{1s}^2$ (strong anchoring conditions) and restricting the result to only terms depending on h we arrive at [14,41]:

$$f_{Sm}^{(T>T_{\rm NA})}[h] = \Big\{ \frac{B_s}{2 q_0^2 \xi \sinh[h/\xi]} \times \big(\exp[-h/\xi] - \cos[\phi]_N \big) \Big\}, \tag{13}$$

where

$$B_s = 2\alpha_0 q_0^2 \xi_{0\|}^2 \varrho_{1s}^2 \tag{14}$$

is the surface compressibility modulus in an overheated FSSF (B_s can be estimated as $B_s \sim B_b$, where B_b is a bulk compressibility). The first term in eq. (13) describes the usual contribution to the free energy due to spatial nonuniformity of the amplitude $\varrho_1(z)$, while the second term corresponds to the elastic deformation energy, which is a penalty for the deviation of the film thickness h from

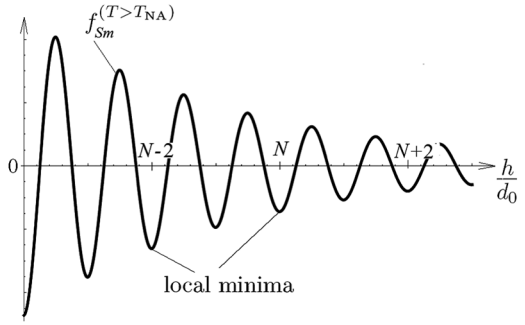

Fig. 2. The h-dependent part (13) of the Landau-de Gennes free energy of the FSSF for the large values of thickness h.

integer values $h_N = Nd_0$. According to eq. (13), the free energy of an overheated FSSF shows an oscillatory dependence on N. There is an infinite number of local minima at $h = h_N$, the depth of which gets smaller with increasing N.

As noted in [14], the oscillatory behavior of the free-energy equation (13) leads to a division of h space in alternating zones, distinguished by the sign of the effective compression modulus (see fig. 2). There are forbidden gaps, where the effective compression modulus is negative ($[f_{Sm}^{(T>T_{NA})}]''_{hh} < 0$), corresponding to absolutely unstable states. Stable zones (or more correctly, metastable ones) occur for $[f_{Sm}^{(T>T_{NA})}]''_{hh} \geq 0$. The width of the allowed zones, centered at $h = h_N$, is limited by

$$|h - h_N| \leq \frac{d_0}{4}\,. \tag{15}$$

Such a behavior is a signature of the metastable thermodynamic state of the overheated smectic film. Indeed, the condition of eq. (15) means that under an external force the thickness of the FSSF can vary continuously only within relatively narrow zone. In any case its variation can not exceed the width of the corresponding allowed zone.

4.2 Equilibrium thicknesses and loss of stability of overheated FSSF

Let us now consider the loss of stability of an overheated FSSF. Determination of the equilibrium values of the FSSF parameters is based on variation of $F_{\rm tot}$, eq. (2). For $h = \text{const}$ at given T (flat part of the film) all terms in eq. (2) with gradients of h over r become zero. Thus, the variation of the free energy is equivalent to minimization of $f[\vartheta, h]$ given by eq. (7). The gravitational term in eq. (2) is negligibly small for the flat part of the film. Following the considerations presented in sect. 3.2, we first vary the free energy of the system (7) over ϑ. Taking eq. (13) into account we arrive at the following condition:

$$p_{Sm}^{(L)} + A\vartheta - C\eta_N + A\kappa\Delta T = p_{\rm air}, \tag{16}$$

where we introduced

$$\eta_N = \frac{[\phi]_N}{q_0 h}\,. \tag{17}$$

Due to the oscillatory character of the free energy, eq. (13), stable thermodynamic states of the film correspond to values of η_N satisfying the condition $-d_0/(4h) < \eta_N < d_0/(4h)$. Accordingly, $\eta_N \ll 1$ due to the condition $h \gg d_0$.

It is widely believed that the pressure in a FSSF is smaller than the external one by an amount determined by the curvature of the meniscus. In our opinion, this is not true and originates from an incorrect interpretation of the shape of the meniscus, see appendix A. In accordance with the arguments presented in sect. 3.2 we can write

$$p_{Sm}^{(L)} = p_{\rm air}, \tag{18}$$

taking into account that during the experiment the external pressure $p_{\rm air}$ is kept constant [8]. Keeping this in mind, the solution of the eq. (16) reads

$$\vartheta = \frac{C}{A}\eta_N - \kappa\Delta T. \tag{19}$$

In parallel, variation of the free-energy equation (7) over h, taking eqs. (13) and (18) into account, leads to

$$\frac{A}{2}\vartheta^2 - C\vartheta + A\kappa\Delta T\vartheta + \frac{\partial f_{Sm}^{(T>T_{NA})}[h]}{\partial h} = 0, \tag{20}$$

where the term $p_{Sm}^{(L)}\vartheta$ is disregarded as being much smaller then $A\kappa\Delta T\vartheta$ term for the whole range of the material parameters of the system used.

Using the inequality (11), we consider in eq. (20) only the main contribution to $\partial f_{Sm}^{(T>T_{NA})}[h]/\partial h$ from (13). Then substitution of eq. (19) into the eq. (20) gives the transcendental equation over η_N, which can be represented in the form

$$\Pi_{Sm}^{(N)}[h] = -\Pi^{(T)}, \tag{21}$$

where

$$\Pi_{Sm}^{(N)}[h] \approx -\frac{B_m^{(N)}}{q_0\xi}\sin[\phi]_N \tag{22}$$

is the main contribution to the elastic restoring force (per unit area) and

$$B_m^{(N)} \approx B_s \exp[-h_N/\xi] \tag{23}$$

is the compression modulus in the middle plane of the overheated smectic film. The force (22) arises in the system when an external force is applied to the free surfaces of the FSSF. In turn

$$\Pi^{(T)} = \frac{C^2}{2A}(\iota - \eta_N)\big(\eta_N + (\iota - 2)\big), \tag{24}$$

is the additional normal force applied to the free surfaces of the film, where we define

$$\iota = \frac{A\kappa\Delta T}{C}\,. \tag{25}$$

According to eq. (24), $\Pi^{(T)}$ is positive if $(2 - \iota) < \eta_N < \iota$. If this is fulfilled, the right part of eq. (21) is clearly negative. This is quite usual for the range of the temperature

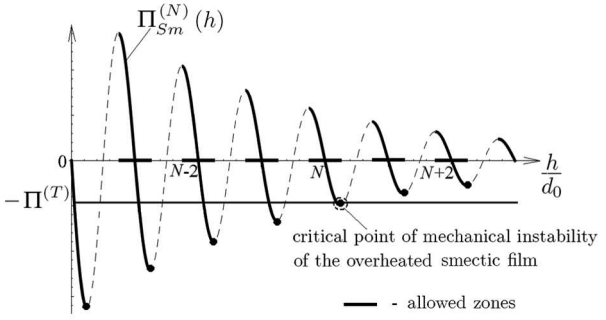

Fig. 3. Balance of forces in a FSSF for large values of the film thickness h. The critical points where the balance of tensile and elastic forces break down are indicated by filled circles. Note that the process of thinning corresponds to a move along the abscissa from the right to the left.

change used. Keeping in mind eq. (12) and the definition of $[\phi]_N$ given after eq. (12), this means that the film is stretched along the layer normal. Thus, sufficiently large heating leads to the stretching of the film along the layer normal[1].

According to eq. (19) the value of ϑ depends on the ratio A/C. Experiments on the second sound in smectics (see for example [42,43]) justify the following inequalities: $C/A \ll 1$ and $C^2A^{-1} \ll B$. However, it is unclear how to specify independently the values of C. Anyway, because $\eta_N \ll 1$, the variation of ϑ is predominately determined by the second term in eq. (19). Hence, eq. (24) for the additional normal tensile force can be simplified to

$$\Pi^{(T)} \approx C\,\kappa\,\Delta T\frac{(\iota-2)}{2}\,. \tag{26}$$

The thickness dependence of the forces acting on the overheated FSSF is shown in fig. 3. The admissible values of h do not exceed the borders of the allowed zones given by the inequality of eq. (15). Because allowed and forbidden zones alternate, the elastic properties of a overheated FSSF are discontinuous functions of the thickness h. The force in eq. (22) has upper and lower limits $[\Pi_{Sm}^{(N)}]_{\pm}^{*} = \pm B_m^{(N)}(q_0\xi)^{-2}$, which are reached at the bottom (+) and top (−) boundaries of the corresponding allowed zones (see fig. 3), given by simply setting $\sin[\phi]_N = \pm 1$ in eq. (22). According to eq. (23), the limiting values of $\Pi_{Sm}^{(N)}$ decrease rapidly with increasing of the overheating τ and increase for a smaller number N of smectic layers (see fig. 3).

Near the minima of the free-energy equation (13), eq. (22) simplifies to $\Pi_{Sm}^{(N)} \approx -B_m^{(N)}(\delta h/\xi)$, where $\delta h = h - h_N$. This agrees with the fact that when the inequalities of eq. (11) hold, the elastic deformation with a thickness of the order ξ is entirely concentrated in the middle of the FSSF, where the bulk modulus ($B_m^{(N)}$) of the pre-smectic density wave is minimal [12].

Evidently, the overheated smectic film remains stable till the point where the balance between the tensile and the elastic restoring force still holds, *i.e.* up to $B_m^{(N)}/(q_0\xi) \geq \Pi^{(T)}$ (see fig. 3).

According to eq. (21), upon further heating the overheated FSSF in the presence of the normal tensile force, the equilibrium value of h shifts continuously toward the upper limit of the corresponding allowed zone, determined by eq. (15). At this point, the balance of tensile and elastic forces breaks down spontaneously, leading to mechanical instability. The balance can be restored as a result of thinning of the film by spillage of excess material into the surrounding reservoir. Generally, a regular series of spontaneous thinning transitions should occur. The upper limit of the allowed zone is the critical point of mechanical instability of the overheated smectic film (see fig. 3). These points (distinguished by an asterisk for clarity) are reached for a critical overheating $\tau^*[h_N^*]$ given by the condition

$$\frac{B_m^{(N)}}{q_0\xi^*} = \Pi^{(T)}, \tag{27}$$

where $\xi^* = \xi_{\|0}(\tau^*[h_N^*])^{-1/2}$. Neglecting the subtle dependence of $\ln[h_{N-1}^*/\xi^*]$ on $\tau^*[h_N^*]$, we get an approximate scaling relation for the points of the maximum overheating of the FSSF from the eq. (27)

$$\frac{h_{N-1}^*}{\xi^*} \approx \text{const}, \tag{28}$$

where the constant can be evaluated as 4. The critical thickness h_{N-1}^* diminishes when the temperature of the film increases because the amplitude of the restoring force decreases with increasing temperature. Due to the power low dependence of $\xi[\tau]$, the envelope of points of maximum possible overheating $\tau^*[h_N^*]$, should be a power function over h_N^*, with an exponent that is inverse to the exponent ω of the bulk smectic correlation length [14]

$$\tau^* \propto \left(\frac{h_{N-1}^*}{\xi_{\|0}}\right)^{-\frac{1}{\omega}}\,. \tag{29}$$

In the mean field approximation $\omega = 0.5$ and therefore $\tau^* \propto (h_{N-1}^*)^{-2}$. Equation (29) is a trivial consequence of the fact that if the inequalities of eq. (11) are valid, the elastic restoring force $\Pi_{Sm}^{(N)}[h]$ is short-range [14]. From eqs. (23) and (22) it is evident that $\Pi_{Sm}^{(N)}[h]$ shows a fast exponential decay with film thickness. As a result, eq. (21) gives with good accuracy a power function h^* over τ^* for the points of maximum possible overheating. The process of discrete thinning of the overheated FSSF has an irreversible, monotropic character, because returning to larger thicknesses on cooling is energetically unfavorable (see fig. 2).

[1] Note that a mechanical tensile force imposed on a homeotropic smectic-A slab leads to a periodic undulation of the layers (Helfrich-Hurault instability, see ref. [16] pp. 364–366). In this situation the smectic layers are clamped at the boundaries and the number of layers is constant, in contrast to the situation in FSSF. Moreover, the heat-induced stress in FSSF (eqs. (24) and (50)) is about 2-3 orders of magnitude smaller.

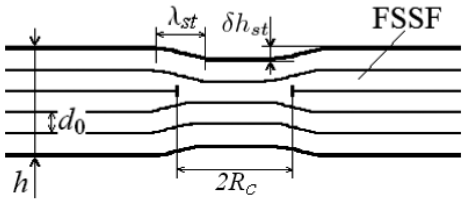

Fig. 4. Schematic representation of an elementary dislocation loop in the middle plane of the free smectic film.

We note that fluctuation-induced interactions (van der Waals and thermal pseudo-Casimir), which are essential for the growth of wetting films [44–48], are negligibly smaller than those considered here and do not contribute to the free energy of the system.

4.3 Dislocation mechanism of thinning

Now we turn to an analysis of the specific mechanism of layer thinning. According to the Landau-de Gennes theory, layer thinning proceeds for an oscillatory free energy of which the amplitude decays with film thickness. Additionally, the internal elastic forces should be balanced by some external tensile (or compressive) stress. However the concrete mechanism by which material from the excess layer moves to the film exterior necessary includes kinetic processes, *i.e.* nucleation and growth of dislocation loops. Note that FSSF are generally remarkably steady within the stability range of the bulk smectic phase [5–8]. As discussed by de Gennes and Prost (see ref. [16], p. 359), in this situation layer-by-layer thinning is impossible because there is no gain in surface energy. For the case of overheated smectic films the situation is different: we do have an energy gain upon going to smaller thicknesses. In this situation the probability of spontaneous thinning becomes rather large [14]. The thinning process is associated with a thermal generation of elementary edge dislocation loops in the middle plane of the film (see fig. 4), where the effective line tension $E_d^{(N)}$ of dislocations is minimal [14,19–21]. If a dislocation loop has a radius smaller than the critical one, it collapses, and if it is larger, it grows and finally merges with the meniscus.

Let us consider the conditions for which formation of an edge dislocation loop in the middle plane of the film might be energetically favorable. The gain in the free-energy density (per unit area of the overheated film, see eq. (7)), due to thinning of the flat part of the film by one layer, has the form

$$\Delta f \approx C\,\kappa\,\Delta T\left\{\frac{[\phi]_{N-1}}{q_0}-\frac{[\phi]_N}{q_0}\right\} + \frac{B_s}{2q_0^2\xi}\left\{-\frac{\cos[\phi]_{N-1}}{\sinh(h_{N-1}/\xi)}+\frac{\cos[\phi]_N}{\sinh(h_N/\xi)}\right\}. \quad (30)$$

Equation (30) suggests that the excess material that goes into the meniscus possesses a bulk nematic phase. Any change of the free energy of the meniscus is negligibly smaller than that of the flat part of the film and does not contribute to Δf. The thinning process changes a FSSF of thickness h_N into one of the thickness $h_{N-1} \approx (N-1)d_0$ with $[\phi]_{N-1} \ll 1$.

Table 1. Typical parameters of the discussed compounds.

Parameter	5O.6	8CB	4O.8
d_0 (10^{-9} m)	2.53[a]	3.17[f]	2.86[c]
B_s (J m^{-3})	$2.5\cdot10^{7}$[b]	$1.09\cdot10^{7}$[b]	$\approx B_b$
K_1 (N)	10^{-11}[c]	10^{-11}[c]	10^{-11}[c]
γ (J m^{-2})	0.02[d]	0.025[g]	0.021[d]
η (N s m^{-2})	10^{-1}[e]	10^{-1}	10^{-1}
λ_p (N s)$^{-1}$	10^{-19}[e]	10^{-19}	10^{-19}
κ (K^{-1})	10^{-3}[h]	$1.1\cdot10^{-3}$[h]	$\sim 10^{-3}$[i]

[a] [8].
[b] [49].
[c] [9].
[d] [9,61].
[e] [16,59].
[f] [62].
[g] [18,25].
[h] Our approximation.
[i] [35,36].

Table 2. Estimations of the values of the first and second terms in eq. (30) for the LC compounds cited in table 1.

Parameter	5O.6	8CB
ΔT (K)	2.95[a]	0.6282[b]
τ	0.0087[a]	0.00205[b]
h_N	$21.25\,d_0$[a]	$84\,d_0$[b]
First term (J m^{-2})	$4.2\cdot10^{-6}$	$\sim 10^{-6}$
Second term (J m^{-2})	$1.9\cdot10^{-6}$	$\sim 10^{-6}$

[a] [8].
[b] [20].

In order to understand the relative contribution of the different terms in eq. (30), we shall make some numerical estimations. The typical parameters of the compounds 5O.6 and 8CB, which will be considered below, are given in table 1. In the following we take $T_0 = T_{\rm NA}$, $C = A\kappa\Delta T/\iota$ (see eq. (25)); the estimation for $\xi_{0\|}$ is taken as $\xi_{0\|} \approx d_0/3$ in analogy with the case of 4O.8 from [50]. Taking for the compound 5O.6 $\iota = 2.5$ and $\iota = 2.01$ for the liquid crystal 8CB, we obtain for the chosen values of ΔT and h_N that the first term (proportional to C) and the second term (proportional to B_s) in eq. (30) are of the same order of magnitude (see table 2). Thus both contributions to eq. (30) have to be taken into account. As usual the energy gain implies that Δf has a negative sign.

The work to produce an elementary dislocation loop of the radius R in the middle plane of the film (see fig. 4) can be written as

$$W = E_d\,2\,\pi\,R + \Delta f\,\pi\,R^2, \quad (31)$$

where the excess line energy E_d of the elementary dislocation is a sum of bulk and surface contributions, E_b and surface E_{st}, respectively

$$E_d = E_b + E_{st}. \tag{32}$$

These quantities are related to the formation of the elastic field of deformation in the film interior and to the appearance at the free surfaces of transitional edge profiles of height $\delta h_{st} \sim d_0/2$, respectively [14, 51–53] (see fig. 4). These surface profiles provide a smooth variation of the film thickness of the order d_0.

The surface contribution E_{st} to the excess line energy of the elementary dislocation can be estimated as follows [14]:

$$E_{st} \simeq 2\gamma \frac{(\delta h_{st})^2}{2\lambda_{st}}\,, \tag{33}$$

where $\delta h_{st} \sim d_0/2$ and the coefficient 2 in the numerator occurs because the edge profiles exist on both free surfaces. The width λ_{st} of the edge profile is determined by the effective width of the distortion produced by the dislocation at the free surface (see [19,54,56] and footnote[2]). Two cases should be distinguished, first $\gamma \gtrsim \sqrt{K_1 B}$, which is valid for bulk smectic, and will be considered below for film thickening (sect. 5.3). Another case $\gamma \gg \sqrt{K_1 B}$ is valid above the bulk NA transition. Here the compression modulus B is taken at the middle plane of the film: $B_m^{(N)}$. Thus $\gamma \gg \sqrt{K_1 B_m}$ and according to (see [19, 54, 56] and footnote[2]) λ_{st} is defined as

$$\lambda_{st} \simeq \sqrt{\pi\, \lambda_m\, h\, \gamma (K_1\, B)^{-1/2}}, \tag{34}$$

where $\lambda_m = \sqrt{K_1/B_m}$ is a smectic "penetration" length [16].

The bulk contribution E_b to the line energy of an elementary dislocation loop can be estimated from result by de Gennes and Kleman for the linear energy of an edge dislocation in smectics [16, 57, 58]

$$E_b \simeq \frac{\sqrt{K_1 B_m^{(N)}}\, d_0^2}{2r_c} + E_c. \tag{35}$$

The core radius r_c can be estimated on the basis of eq. (34) taking $h = \xi$, *i.e.* $r_c \sim \sqrt{\pi \lambda_m \xi \gamma (K_1 B_m)^{-1/2}}$. The core energy of an elementary dislocation E_c can be estimated as $\sim 0.1\sqrt{K_1 B_m^{(N)}}\, d_0^2/(2r_c)$ [59], a typical value for the core energy in solid materials. Generally, the calculation of the core energy E_c of dislocations in smectics is a complicated task that has been performed only for some specific cases (see for example ref. [60]).

Finally, from eq. (31) the activation energy of the dislocation loop of the critical radius can be expressed as

$$W^{(cr)} = -\pi \frac{(E_d)^2}{\Delta f}\,. \tag{36}$$

[2] The above formalism of dislocation formation and growth is not only applicable to smectic liquid crystals, but also to other lamellar systems, for example formed in block-copolymers [55].

Table 3. Estimations of the values of E_b and E_{st} for the LC compounds cited in table 1

Parameter	5O.6	8CB
ΔT (K)	$2.95^{(a)}$	$13^{(b)}$
τ	$0.0087^{(a)}$	$0.0424^{(b)}$
h_N	$21.25\, d_0{}^{(a)}$	$11\, d_0{}^{(b)}$
E_b (J m^{-1})	$2.15 \cdot 10^{-13}$	$1.78 \cdot 10^{-13}$
E_{st} (J m^{-1})	$0.7 \cdot 10^{-13}$	$0.89 \cdot 10^{-13}$

(a) [8].
(b) [20].

To calculate the value of $W^{(cr)}$ we need to know the relative contributions to E_d from E_b and E_{st} (see eq. (32)). These can be estimated using eqs. (33) and (35) and the parameters of the liquid crystals 5O.6 and 8CB cited in table 1. The results for chosen values of ΔT and h_N are presented in table 3. The value of E_b turns out to be few times less than E_{st}, and we have to take both terms into account.

Using an approach proposed by Langer and Fisher [63] (see also [51]), the frequency of thermal nucleation of a smectic dislocation loop can be expressed as

$$\nu \cong \nu_0 \exp\big[-W^{(cr)}/(k_B T)\big], \tag{37}$$

where ν_0 is a characteristic frequency (rate) for medium perturbation. Thus the average time needed to nucleate one growing loop in a unit area is $\delta t \approx \nu^{-1}$. According to Pershan, Prost and de Gennes [16,51] the order of magnitude of $\nu_0 \approx 10^{26}\,\mathrm{s}^{-1}\,\mathrm{cm}^{-2}$ can be estimated by dividing the sound velocity by both the molecular dimension and cross area.

Finally the expression for ν can be rewritten as

$$\widetilde{\nu} \cong \exp\big[(W_c^* - W^{(cr)})/(k_B T)\big], \tag{38}$$

where $\widetilde{\nu} = \nu \cdot (1\,\mathrm{s} \cdot 1\,\mathrm{cm}^2)$ is the number of thermal nucleations during one second per $1\,\mathrm{cm}^2$, $W_c^* \approx \ln[\widetilde{\nu}_0] k_B T$ is a "threshold" activation energy ($W_c^* \approx 60 k_B T \sim 2.5 \cdot 10^{-19}\,\mathrm{J}$) and $\widetilde{\nu_0} = \nu_0 \cdot (1\,\mathrm{s} \cdot 1\,\mathrm{cm}^2)$. The condition for nucleation of one dislocation loop of critical radius in $1\,\mathrm{s}$ over $1\,\mathrm{cm}^2$ is then $W^{(cr)} = W_c^*$. For $W^{(cr)} \lesssim W_c^*$ the probability for nucleating of the dislocation loops is high, while for $W^{(cr)} > W_c^*$ it is negligible.

Next we calculate the probability of the thermal generation of dislocation loops near the critical points where the balance of forces breaks down, for which $[\phi]_N \approx q_0 d_0/4$ and $\cos[\phi]_N = 0$. Taking as estimates the parameters of thinning for the liquid crystal compound 5O.6 from table 3 we get from the equilibrium condition (21) that $[\phi]_{N-1} \approx 0.79$ and $W^{(cr)} \approx 0.26 \cdot 10^{-19}\,\mathrm{J}$. This value is about five times smaller than the activation energy W_c^*, hence the probability for nucleating of dislocation loops is really high. This mechanism can easily provide the discrete (layer-by-layer) thinning of overheated FSSF.

On the other hand, close to points of integer values of the film thickness ($h_N \approx 21 d_0$ for $\Delta T = 2.7\,\mathrm{K}$ [8]), for which $[\phi]_N \approx [\phi]_{N-1} \approx 0.79$, we get $W^{(cr)} \approx 5.75 \cdot 10^{-19}\,\mathrm{J}$.

Therefore, evidently far away from the critical points of loss of mechanical stability $W^{(cr)} > W_c^*$, and the probability of spontaneous nucleation of growing dislocation loops is vanishingly small. The estimations for liquid crystal 8CB give the similar results.

4.4 Envelope of the actual points of thinning

In this section we derive an approximate equation for the envelope of the actual points where the thinning transitions take place. We recall that earlier we deduced the envelope of critical points of the loss of stability of overheated FSSF (see eq. (29)). These points were designated with an asterisk ($\tau^*[h_N]$) and correspond to maximum overheating possible for a film of given thickness h_N^*. To determine the actual points of thinning, the probability character of nucleation has to be taken into account. To be more precise, we should calculate the probability of generating a dislocation loop near the critical points where the mechanical balance of the film is lost. Keeping only the surface contribution E_{st} to the linear dislocation energy E_d,

$$W^{(cr)} \simeq -\frac{\gamma d_0^3 B_s}{16\Delta f}\frac{d_0}{\xi}\frac{\xi}{h_{N-1}}\frac{1}{\sinh[h_{N-1}/\xi]}\,. \qquad (39)$$

Furthermore, from eq. (39), using the condition $W^{(cr)} = W_c^*$, and having in mind that $\Delta f \simeq -C\kappa\Delta T[\phi]_N q_0^{-1}$, $\sinh[h_{N-1}/\xi] \approx (1/2)\exp[h_{N-1}/\xi]$, we get

$$\frac{h_{N-1}^{(r)}}{\xi} \simeq \ln\frac{\gamma d_0^2 B_s \iota}{2W_c^* A(\kappa\Delta T)^2}\frac{d_0}{\xi} + \ln\frac{\xi}{h_{N-1}^{(r)}}\,. \qquad (40)$$

The subtle logarithmic dependence on the right side of eq. (40) on $h_{N-1}^{(r)}\xi^{-1}$ (and thus on τ) means that this part can be considered as a temperature-independent constant. As a result we obtain the same scaling relation as found earlier for the envelope $\tau^*[h_N]$ (eq. (28)):

$$\frac{h_{N-1}^{(r)}}{\xi} \approx \text{const.} \qquad (41)$$

Remarkably, the const in eq. (41) has a value ≈ 3.1, close to the value 4 calculated for eq. (28). The envelopes of the actual thinning transitions and of the critical points are compared in fig. 5.

The envelope of the points of actual thinning does not exceed the $\tau^*[h_{N-1}^*]$ as required (see fig. 5). This situation would occur if the value of $\exp[h_{N-1}^{(r)}/\xi]$ as determined from condition $W^{(cr)} = W_c^*$ is lower than $\exp[h_{N-1}^*/\xi^*]$ obtained from eq. (27). This is the case if

$$\Pi^{(T)} < \frac{4W_c^* A(\kappa\Delta T)^2}{\gamma d_0^2 \iota}\frac{h}{d_0}\frac{1}{q_0\xi}\,. \qquad (42)$$

The inequality of eq. (42) determines the conditions for which a cascade of thinning transitions can be accomplished.

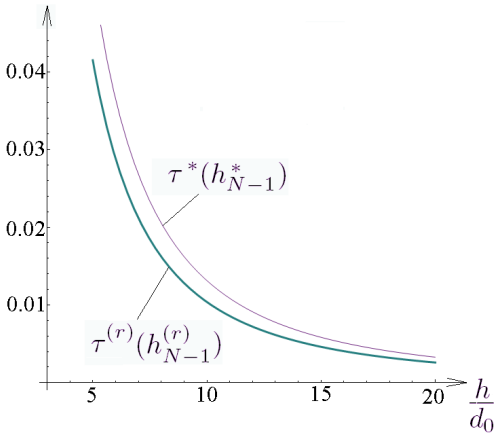

Fig. 5. Schematic representation of the envelope $\tau^{(r)}[h_{N-1}^{[r]}]$ of the points of the actual thinning transitions and the envelope $\tau^*[h_{N-1}^*]$ of the critical points of mechanical instability of FSSF.

Let us make some estimates for the parameters of thinning transitions for a 53 nm thick FSSF of the liquid crystal 5O.6, for an overheating of $\Delta T \approx 2.95\,\text{K}$ (see tables 1, 3). First, from eq. (26) we have for $\Pi^{(T)} \sim 0.66 \cdot 10^4\,\text{J m}^{-3}$, then according to eq. (27) the compression modulus on the envelope of the critical points should be $B_m^{(N)} \simeq 1.52 \cdot 10^5\,\text{J m}^{-3}$. This gives for the overheating an equilibrium film thickness $h_N \approx 4.87 \cdot 10^{-8}\,\text{m}$ or $h_N \approx 21 d_0$, which is in good agreement with experiment [8].

The dynamics of the growth of dislocation loops during thinning has been studied in various papers [18–21,23]. An appropriate technique was originally developed by Geminard *et al.* [18], and consists of a folded heating wire placed close to the film. Application of a heat pulse overheats the FSSF locally into the nematic or isotropic phase. This generates in the middle plain an elementary dislocation loop that moves in the direction of the meniscus. The velocity of the dislocation loops was determined to be of the order of $v_{dl} \sim 10^{-6}\,\text{m s}^{-1}$. This means that in order to reach the edges of the frame, typically at a distance of $\sim 10^{-3}\,\text{m}$, the dislocation needs about $10^3\,\text{s}$. Accordingly, to observe layer-by-layer thinning steps in an overheated FSSF, the heating rate should not exceed this value. Such conditions were fulfilled, for example, in an experiment by Dolganov *et al.* [8] on FSSF of 5O.6, in which the heating rate was $\sim 10^{-3}\,\text{K s}^{-1}$. The characteristic times of the thinning process will be discussed in sect. 6.

Finally we note that thinning of FSSF occurs systematically in the process of their creation. During stretching of a FSSF a stress is applied in the plane of the film, which favors the formation of dislocations and further thinning of the film. The physics of creation of a FSSF is discussed in appendix B.

4.5 Formation of droplets

Let us consider now the situation of an overheated smectic film if the inequality eq. (42) does not hold. In this case the

formation of dislocation loops is unfavorable, even though the balance of forces is disrupted. Hence the system remains in the metastable state. Discrete thinning transitions should not occur and instead nematic or isotropic droplets have been observed [64–68]. It is not accidental that the appearance of such droplets is observed in materials for which the layer thinning is not found [68].

Upon exceeding the critical point, the pressure difference $\delta\Pi$, due to failure of the balance of forces, is small. For an estimate, let us assume that the nematic or isotropic droplet formed in the middle plane of the FSSF has a flat central part and a height of the order of d_0. At the edges there is a transitional profile of width λ_{st} (34). Hence we may assume that the excess line energy associated with the droplet is given by eq. (33). The gain in free energy (per unit volume) due to the formation of a nematic (isotropic) droplet in the overheated FSSF has the form

$$\Delta f_{dr} \approx -C\,\kappa\,\Delta T\,\frac{[\phi]_N}{q_0} - \delta\Pi d_0. \tag{43}$$

The main contribution is given by the second term, caused by the pressure difference due the disruption of the force balance. In analogy to eq. (36), the work needed for nucleation of a critical droplet can be written as $W_{dr}^{(cr)} \simeq -\pi E_{st}^2/\Delta f_{dr}$. Let us make some estimates. Suppose that the film is overheated above $T_{\rm NA}$ by 3.8 K, $\iota \approx 3$ and $\delta\Pi \lesssim C\kappa\Delta T(\iota-2)/2$. Then we find that the magnitude of the critical work is about 10^{-20} J, that is less than W_c^*. Thus the formation of a planar droplet is highly probable. Subsequently, another droplet can be formed in the middle of the FSSF and the process can be repeated many times leading to a macroscopic drop.

Nematic drops formed at the NA-transition temperature are convex [64–68] (see also [40,69,70]). This indicates that the pressure in the drop exceeds the external pressure and confirms our initial statement that the pressure in a smectic (nematic, isotropic) liquid is larger than (or equal to) the external pressure (sect. 3.2).

4.6 Thinning at the smectic-isotropic transition ($T > T_{IA}$)

As mentioned above, the first observations of thinning transitions were actually made at the smectic-isotropic (IA) transition of partially fluorinated liquid-crystalline compounds [5, 22, 23]. Later these observations were extended to nonfluorinated mesogens, for example 54COOBC [71]. This indicates that thinning at the smectic-isotropic transition is rather universal. Remarkably, now the smectic layers of the overheated FSSF coexist with an isotropic meniscus possessing only a few smectic surface layers.

The smectic-isotropic transition is first-order due to the interactions between the positional and orientational order parameters. However, upon overheating, the corresponding local minimum in the free energy disappears and the system can be described by eq. (10), the same quadratic functional as used earlier for the smectic-nematic transition. The definition of the correlation length ξ is clearly different from the one at the smectic-nematic transition: it diverges not at the phase transition point, but at some lower virtual temperature. The pre-smectic effects related to confinement of the film at the free boundaries are still strong enough, despite the fact that the bulk transition is first-order. This means that at relatively large overheating, the predictions for the smectic-nematic transition will be also valid for smectic-isotropic.

5 Thickening of FSSF ($T < T_{NA}$)

5.1 Free energy of the flat part of a FSSF

In this section we start the discussion of the effect of thickening in FSSF, which can occur for $T < T_{\rm NA}$. At first glance this process seems to be similar to thinning. In both cases a change of the number of smectic layers proceeds through nucleation and growth of dislocation loops which becomes energetically favorable. However, there is a fundamental difference. Layer-by-layer thinning of overheated films originates from the oscillating character of the free energy of the system that leads to forbidden zones. In the case of thickening such forbidden zones are absent and the origin of the effect is different.

A FSSF stretched on a frame is in mechanical equilibrium due to the elastic response of the layers and the support from the meniscus. Local heating of the smectic film (either by absorption of an evanescent X-ray wave [15] or by some other means [32]) causes additional stress. This leads to extra contributions to the free-energy density of the system that shift the heated volume to a metastable state. The main contribution arises from local thermal expansion of the smectic film as described by a second and third terms in our general eq. (7). In the following we show that for relatively large heating nucleation and growth of dislocation loops of the excess smectic layers becomes energetically favorable and thus probable. The material, necessary for the film to thicken, flows from the meniscus to the volume under the illuminated area.

To describe the effects mentioned above, we use eq. (7) from sect. 3.2 augmented by the expression for the excess Landau-de Gennes free energy per unit area of the film $f_{Sm}[h]$ for $T < T_{\rm NA}$ given by (8) with $\tau = -|\tau|$. The value of the order parameter that minimizes the bulk functional in an infinite medium is given by

$$\varrho_{0b}^2 = \frac{\alpha_0|\tau|}{\beta}\,. \tag{44}$$

In a film of finite thickness h at temperatures below $T_{\rm NA}$, the order parameter ϱ_1 is slightly larger than the bulk value ϱ_{0b} because of the presence of two free surfaces

$$\varrho_1 = \varrho_{0b} + \delta\varrho, \tag{45}$$

where $|\delta\varrho| \ll \varrho_{0b}$. After substitution of eq. (45) in eq. (8) we minimize the expression with respect to $\delta\varrho(z)$ and $u(z)$.

After integration over z we arrive finally at a h-dependant contribution to the excess of the free energy far away from the meniscus

$$f_{Sm}^{(T<T_{\rm NA})}[h] = \left\{ -\frac{B_b\, h}{8(q_0\,\xi)^2} + \frac{\delta B_s}{\sqrt{2}\, q_0^2\, \xi} \tanh\left[\frac{h}{\sqrt{2}\,\xi}\right] + \frac{B_b}{2}\left(\frac{h - N\, d_0}{N\, d_0}\right)^2 h \right\}. \quad (46)$$

Here $\xi = \xi_{\|0}|\tau|^{-1/2}$ is the bulk value of the smectic longitudinal correlation length, $\delta\varrho(z = \pm h/2) = \delta\varrho_s$, $B_b = 2\alpha_0 q_0^2 \xi_{0\|}^2 \varrho_{0b}^2$ is the bulk compressibility modulus, and $\delta B_s = 2\alpha_0 q_0^2 \xi_{0\|}^2 (\delta\varrho_s)^2$ is the surface contribution to be added to the bulk modulus. For comparison with experiment we shall use the estimate of the bulk compression modulus B_b from its empirical temperature dependence for the liquid-crystal compound 4O.8 in ref. [49]

$$B_b \approx 0.7|\tau|^{0.7} \cdot 10^9\, \mathrm{J\,m^{-3}}. \quad (47)$$

Because $\delta\varrho_s \ll \varrho_{0b}$, and thus $\delta B_s \ll B_b$, the contribution from the surface term in the free-energy equation (46) can be neglected.

The next step is to take the change in the external conditions of the system into account, in our case the local heating of the film. To do this, eq. (46) for the free energy of the FSSF should be substituted in the general eq. (7). The resulting free energy is a function of the mean density deviation ϑ and the thickness h of the film, that both depend on the temperature variation ΔT as an external parameter.

5.2 Stretching of a FSSF along the layer normal due to local heating

Similarly to the case of film thinning, we consider the flat part of the film (h = const at given T) and neglect the effect of gravitation. Thus, the variation of the free energy is equivalent to minimization of $f[\vartheta, h]$ given by eq. (7). In the following we will consider the general case when $p_{Sm}^{(L)}$ deviates from pressure of the surrounding gas, $p_{\rm air}$, by an amount Δp (see eq. (9)). Variation of the free energy of the system eq. (7) with respect to h, taking eqs. (9) and (46) into account, gives the following equilibrium condition of the system:

$$\frac{A}{2}\vartheta^2 - C\vartheta + A\kappa\Delta T\vartheta - \Delta p - \frac{B_b}{8(q_0\xi_b)^2} + B_b\left(\frac{h - Nd_0}{Nd_0}\right) = 0. \quad (48)$$

As before, we keep only the leading terms. Similarly to eq. (25), we introduce the parameter ι, and suppose that $C \lesssim 10^{-1}B$. Then we arrive at the condition $\eta_N \ll 2 < \iota$, which is valid for the whole range of temperature changes in the film. The first reaction of the FSSF to local heating will be a change of the mean density (see sect. 3.2). This means that we can consider the local heat expansion of FSSF in analogy with eq. (19) as due to changes of the mean density of the film

$$\vartheta \approx -\kappa\Delta T, \quad (49)$$

where $\Delta T = T - T_0$ and $T_0 = T_{\rm NA} - 13.5\,\mathrm{K}$. Substitution of eq. (49) into the eq. (48) gives, after some simple algebra, the transcendental equation over η_N, which can be written in the form

$$B_b\eta_N = \Delta p + \frac{B_b}{8(q_0\xi_b)^2} + \frac{C^2}{2A}\iota(\iota - 2), \quad (50)$$

where

$$\eta_N = \left(\frac{h - Nd_0}{Nd_0}\right). \quad (51)$$

In compliance with the inequalities quoted above, the right part of eq. (50) is positive. This means that $\eta_N > 0$ and smectic layers are stretched along the layer normal. Thus, similarly to the case of overheated films, local heating of the FSSF leads to the appearance of normal tensile stress (see footnote[1]).

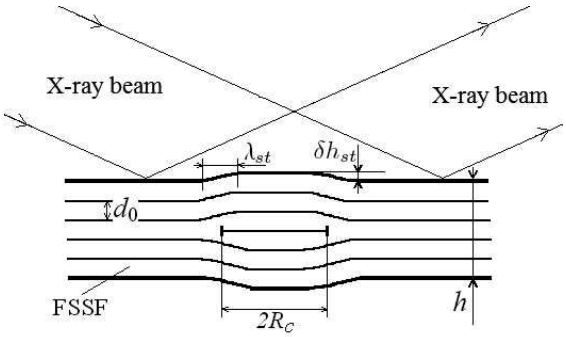

Fig. 6. Sketch of an elementary dislocation loop of the excess smectic layer in the middle plane of the free smectic film.

5.3 Dislocation mechanism of thickening of FSSF

As in any layered system, discrete changes of the film thickness can only proceed by thermal generation of elementary edge dislocation loops [55,59]. Then the question arises whether the energy gain associated with formation of an excess smectic layer is large enough to make the generation of loops favorable. To answer this question we calculate the activation energy of an elementary dislocation loop of critical radius associated with an excess smectic layer, to be compared with the threshold energy W_c^* (see after eq. (38)).

Before proceeding further let us discuss in some detail how we model the experimental situation (see fig. 6). As described in the experiment of de Jeu *et al.* [15], specific heating conditions apply to thickening of a FSSF. The films were irradiated by X-rays below the critical angle for total reflection (see sect. 2). The energy dissipation is due to absorption of X-rays at one side of the film. The heating is strongly localized at the surface because the intensity of the evanescent X-ray wave decays exponentially

along the film normal. However, heat diffusion across the film is very fast (see appendix C). Accordingly, the temperature gradient along the film normal is very small. In combination with the limited thickness of the film (tens of nm) we can neglect the initial asymmetry on the timescale of the thickening. Note that in the plane of the film the dimensions are orders of magnitude larger and in comparison lateral heat diffusion will be slow (appendix C). Hence we arrive at the model depicted in fig. 6. Below the footprint the film is effectively uniformly heated while the meniscus and the part of film adjacent to it stay at the original temperature. Dislocation loops of an excess smectic layer are thermally generated in the middle plane of the film as should be for the compound 4O.8 in the temperature range of smectic phase used[3]. As a consequence the thickening will occur at both sides of the FSSF.

We shall use eq. (31) for the activation energy of the dislocation loop of the excess smectic layer and eq. (32) for the dislocation excess line energy E_d. For the surface contribution to the excess line tension E_{st} we use eq. (33), in which the width of the transition edge profile λ_{st} (see fig. 6) is determined as [19,54–56]

$$\lambda_{st} \simeq 2\sqrt{2\,\pi\,\widetilde{\lambda}\,h}, \tag{52}$$

and is valid for bulk smectic where $\gamma \gtrsim \sqrt{K_1 B}$ and $\widetilde{\lambda} = \sqrt{d_0^2 + K_1/B}$. The quantity $\widetilde{\lambda}$ differs from the "penetration" length λ used for $T \gtrsim T_{\rm NA}$ (see sect. 4.3) due to saturation of λ in the smectic phase far away from the smectic-nematic transition [72–74]. To calculate the "bulk" contribution E_b to the line energy E_d we can use eq. (35), where the compression modulus $B_m^{(N)}$ should be replaced by B, the value at the current temperature. For the core radius r_c we use eq. (52) taken for $h = \xi$ at the current temperature, *i.e.* $r_c \sim 2\sqrt{2\pi\widetilde{\lambda}\xi}$.

Thus the expression for the work needed to form an elementary dislocation loop of the excess smectic layer can be written as

$$W = 2\,\pi\,R(\Delta E_{d\,\rm men} + E_d) + \Delta f\,\pi\,R^2, \tag{53}$$

where R is the radius of the loop, Δf is the gain in the free-energy density (per unit area), (see eq. (7)), related to the formation of an elementary dislocation loop of the excess smectic layer in the middle plane of the film, and $\Delta E_{d\rm men}$ is the decrease of the line energy of the dislocation ensemble in the meniscus. $\Delta E_{d\rm men}$ is related to the flow of the material from the meniscus. Because the size of the critical nuclear of the excess smectic layer is too small to produce the disappearance of a whole dislocation loop from the meniscus, $\Delta E_{d\rm men}$ is determined purely by surface contribution $\Delta E_{st\rm men}$. The latter is much smaller then the excess line energy of a critical dislocation loop and can be disregarded. Finally the critical work of the formation of a dislocation nucleus of critical radius is again given by eq. (36). Note that changes of the bulk energy of the meniscus via flow of material have not been considered in sect. 4.3 for overheated films because in the latter case the film coexists with either a nematic or an isotropic meniscus.

To derive an expression for Δf we consider the thickening as a discrete process in which successive excess smectic layers are generated. We denote the associated time intervals of heating by δt. Furthermore, we have to take into account that in addition to heating of the footprint volume there is also partial cooling due to inflow of "cold" material from the meniscus. Hence we introduce the following notations: T_{ij} is the temperature of the film volume under footprint before j-thickening (i is the number of the time intervals counted from the beginning of the heating process, j is the number of the successive layer thickening); $T_{ij}^{(c)}$ is the diminished temperature of the film volume after nucleation of the dislocation loop of the j-th excess smectic layer and the corresponding cooling of the film. Accordingly, $\Delta T_{ij} = T_{ij} - T_0$, T_0 is the initial temperature of the FSSF, $\Delta T_{ij}^{(c)} = T_{ij}^{(c)} - T_0$.

Using eqs. (2), (7), (46), (49) and (51), we can derive expression for Δf, which takes the form:

$$\begin{aligned}\Delta f \approx{}& 2\,\frac{{\rm d}\gamma}{{\rm d}T}\left(T_{ij}^{(c)} - T_{ij}\right)\\ &- \frac{B_b^{(c)}\,h_j}{8(q_0\,\xi^{(c)})^2} + \frac{B_b\,h_{j-1}}{8(q_0\,\xi)^2} + \frac{B_b^{(0)}\,d_0}{8(q_0\,\xi_b^{(0)})^2}\\ &- \frac{A}{2}\,\kappa^2\left(\left(\Delta T_{ij}^{(c)}\right)^2 h_j - (\Delta T_{ij})^2 h_{j-1}\right),\end{aligned} \tag{54}$$

where the contribution from $-p_{Sm}^{(L)}\kappa(\Delta T_{ij}^{(c)}h_j - \Delta T_{ij}h_{j-1})$ has been omitted as it is much smaller then the last term in eq. (54) proportional to A for the whole range of the temperature changes of the film. The first term in eq. (54) accounts for the variation of γ with temperature: $\partial\gamma/\partial T \sim -10^{-5}\,{\rm J\,m^{-2}\,K^{-1}}$, as usually applied for the systems with heterogeneous heating [75]. Furthermore, ξ is the current smectic correlation length, $\xi^{(c)}$ and $B_b^{(c)}$ are the correlation length and compression modulus after nucleation of the dislocation loop, respectively; h_{j-1} and h_j are the thicknesses of the film below the footprint before and after nucleation of the dislocation loop of the excess smectic layer, respectively. The $B_b^{(0)}$ and $\xi_b^{(0)}$ are the bulk compression modulus and smectic correlation length in the meniscus.

Let us analyze the effect of the various contributions to eq. (54) keeping in mind that the total energy gain Δf should be negative. Simple estimates indicate that the first term in eq. (54) is positive and inessential. Regarding the next three terms, small changes in temperature will lead to a certain compensation of the positive and negative terms and the result is small positive. Accordingly, the main gain in the free energy of eq. (54) upon local heating is provided by the last contribution. This term is clearly negative because of the negative sign in front, while the difference in

[3] We recall that dislocations in smectics are nucleated in the middle plane of the film if $\gamma > \sqrt{K_1 B}$, while in the opposite case this happens at the film surface [52, 54–56]. For the liquid crystal 4O.8 considered, the condition $\gamma > \sqrt{K_1 B}$ is well satisfied in the range of smectic phase used.

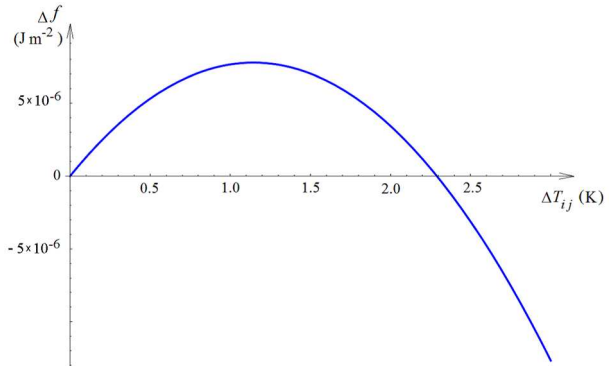

Fig. 7. Schematic presentation of the dependence of the critical energy Δf as a function of ΔT_{ij}.

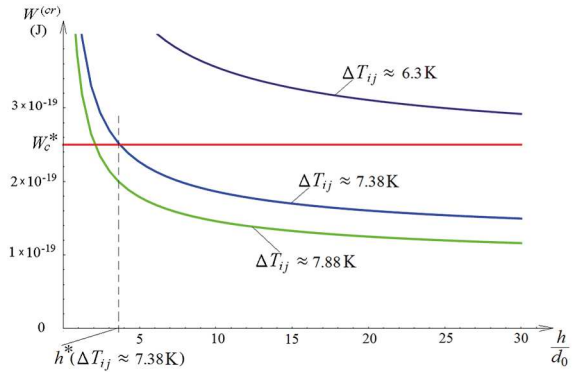

Fig. 8. Schematic presentation of the dependence of the critical energy $W^{(cr)}$ as a function of h for different ΔT_{ij}. The threshold value of h for each ΔT_{ij} ($h^*(\Delta T_{ij})$) can be found from the intersection between curves $W^{(cr)}$ and W_c^*.

the brackets is positive because h_j exceeds h_{j-1} by d_0 and the decrease of $\Delta T_{ij}^{(c)}$ relative ΔT_{ij} is rather small. Thus, the last term in eq. (54) ensures an energy gain to be associated with the process of film thickening. As a result it is energetically favorable for material from the meniscus to move into the heated footprint area.

According to eq. (54) a decrease of ΔT_{ij} leads to a reduction of the absolute value of Δf. At a certain value of ΔT_{ij} the gain in total free-energy density of the system due to the formation of a dislocation loop becomes zero and for smaller ΔT_{ij} it becomes positive, see fig. 7. This indicates the absolute end of the thickening regime. For the parameters used this occurs at $\Delta T_{ij} \approx 2.3\,\mathrm{K}$.

In the following we restrict ourselves to the four-layer film [15] for which $\delta t = 1\,\mathrm{s}$ (see appendix C). We find that conditions for generation of the first dislocation loop of the critical radius appear only after the third second of heating. At that moment $\Delta T_{31} = 7.38\,\mathrm{K}$ (see eq. (C.2) in appendix C). After generation of a dislocation loop of radius R the heat accumulated in the volume surrounding the loop is redistributed due to the enhanced footprint volume. As a result the temperature difference between the footprint volume and the cold part of the film decreases to $\Delta T_{31}^{(c)}$ as given by eq. (C.3). Finally, after substitution of ΔT_{31} and $\Delta T_{31}^{(c)}$ into eq. (54), using the material parameters given in table 1 and taking eq. (53) into account, we can estimate the work of formation of the first dislocation loop $W_{31}^{(cr)} \approx 2.33 \cdot 10^{-19}\,\mathrm{J}$ (for which $R_c \approx 1.8 \cdot 10^{-8}\,\mathrm{m}$). This value of $W_{31}^{(cr)}$ is smaller than the barrier activation energy W_c^* ($W_c^* \approx 60 k_B T \sim 2.5 \cdot 10^{-19}\,\mathrm{J}$, see sect. 4.3 after eq. (38)). The probability for nucleation is large and formation of a first excess smectic layer under the beam footprint is energetically favorable. We note that for this temperature the condition mentioned in footnote[3] is satisfied. The same is true for all other excess layer generations.

Subsequently, after the fourth second of heating, we can calculate the temperature difference $\Delta T_{42} = 7.77\,\mathrm{K}$ between footprint volume and the surrounding film (see eq. (C.4)). Similarly to eq. (C.3) we get an expression for $\Delta T_{42}^{(c)}$, given by eq. (C.5). For the parameters of dislocation loop we obtain $R^{(cr)} \sim 1.5 \cdot 10^{-8}\,\mathrm{m}$ and $W_{42}^{(cr)} \approx 1.82 \cdot 10^{-19}\,\mathrm{J}$. Thus $W_{42}^{(cr)}$ turns out to be smaller than W_c^* and the formation of a second excess smectic layer is also energetically favorable. The value $W_{42}^{(cr)}$ is smaller than $W_{31}^{(cr)}$ and this tendency continues upon further heating. Starting from the third second of heating, the process of layer-by-layer thickening is reproduced systematically.

5.4 Estimate of the final thickness

Now, let us specify the conditions under which successive (layer-by-layer) thickening of a four-layer FSSF can proceed. To do this we restrict ourselves to the essential contributions in eq. (54) and take into account that after nucleation of a dislocation loop of critical radius the temperature decrease in the footprint volume is small enough (compare (C.6) and (C.7)). Thus, we assume $T_{ij} \approx T_{ij}^{(c)}$, and the expression for the activation energy, eq. (53), of a dislocation loop of critical radius can be written in simplified form as

$$W^{(cr)} \approx -\pi \left(\gamma \frac{d_0^2}{8\sqrt{2\,\pi\,\widetilde{\lambda}\,h}} + \frac{\sqrt{K_1\,B_b}\,d_0^2}{4\sqrt{2\,\pi\,\widetilde{\lambda}\,\xi}} \right)^2 \times \left\{ -\frac{B_b\,d_0}{8(q_0\,\xi)^2} + \frac{B_b^{(0)}\,d_0}{8(q_0\,\xi_b^{(0)})^2} - \frac{A}{2}\,d_0\,(\kappa\,\Delta T_{ij})^2 \right\}^{-1}. \quad (55)$$

According to eqs. (55), (C.6) and (C.7), with increasing number of successive intervals of heating and thickening of the film the magnitude of the critical activation energy $W^{(cr)}$ decreases. For example, after the third second of heating the temperature difference ΔT_{31} is approximately equal to 7.38 K. We can plot the dependence of the critical energy $W^{(cr)}$ as a function of h for $\Delta T_{ij} = \Delta T_{31}$ (see fig. 8). For the current thickness of the film under the footprint $h \approx 4d_0$ the value of the critical energy $W^{(cr)}$ is smaller than the threshold activation energy W_c^*. This means that at completion of the third second of heating formation of the first dislocation loop becomes favorable.

The meaning of fig. 8 is straightforward. At each given ΔT_{ij} there is a threshold thickness h^* dividing the regime

of nucleation of a critical dislocation loops from the regime in which this is impossible. If for the conditions of the experiment the initial film thickness exceeds h^*, thickening by one or more layers will occur. On the other hand, if $h < h^*$, the thickness of the film will not change. Consequently, if during the experiment ΔT_{ij} diminishes, the critical thickness becomes so large that current thickness will certainly be smaller than h^*. This indicates termination of the thickening process. If ΔT_{ij} falls below 2.3 K (see fig. 7) this will lead to the absolute end of the thickening. Note that the current calculations should not be mixed up with those from the preceding sect. 5.3. The latter ones are exact calculations based on the heat balance in the system; while the data presented in fig. 8 are semi-qualitative calculations based on eq. (55), and are shown for clearer insight.

In summary, after the third second of heating the thickness of the four layer film increases by one layer during the next second. Starting from this point, the thickness of the FSSF increases by one layer during each second. If, for example, we heat the film during 60 seconds, at the end of this process the thickness of the FSSF has increased by 57 layers and reaches $61d_0$. After the heating is disrupted the temperature of the film volume under the footprint is still large enough ($\Delta T_{60\,58} \approx 10.8\,\mathrm{K}$) for thickening to continue. During this process the value of ΔT_{ij} decreases to about $\Delta T_{ij} \approx 6.0\,\mathrm{K}$. According to fig. 8 the decrease of ΔT_{ij} leads to an increase of the threshold thickness h^*. At a certain point the actual film thickness becomes smaller than the threshold value which indicates the end of the thickening process. We find that this occurs at value of $h \approx 112d_0 \div 113d_0$. These considerations explain the observation in ref. [15] of thickening by many tens of layers.

If the heating time is not limited (still below the angle of total reflection $\alpha < \alpha_c$) eventually the film thickness under the footprint of the beam will grow infinitely (of course, only if we do not overheat the film into the nematic or isotropic phase).

Now the question arises: what will happen with a film of initial thickness larger than four layers under similar conditions. To be more specific let us consider a FSSF with an initial thickness an order of magnitude larger, $h_0 \approx 40d_0$. According to eqs. (55), (C.6) and (C.7) the conditions for generation of the first dislocation loop of the critical radius appear only after 27 seconds of heating. At that moment $\Delta T_{27\,1}$ equals 6.44 K. Consequently, after 60 seconds of heating the thickness of FSSF increases by 33 layers and becomes $73d_0$.

In the transmission regime, $\alpha > \alpha_c$, the heat yield from the X-ray beam is about six times less than in the case of a fully reflected beam with an associated evanescent wave [15]. Then the increase of the initial temperature under footprint is of the order of 1 K/s only. According to fig. 8 the decrease of ΔT_{ij} leads to an increase of the threshold thickness h^*. At these heating values the actual film thickness is smaller than the threshold thickness, which indicates that the thickening process cannot take off. According to our estimates the corresponding value of the critical activation energy is about $W^{(cr)} \sim 4 \cdot 10^{-18}\,\mathrm{J}$, much larger then the threshold activation energy W_c^*. Thus the probability of spontaneous nucleation of growing dislocation loop is vanishingly small and thickening is absent.

To finish this section we remark that the experiments on thickening of FSSF are fundamentally different from the ones using local heating by a heating wire [18,19,21,23]. In latter case the film is heated locally up to a transition to the nematic or isotropic phase. Estimates based on the parameters of heating from ref. [18] indicate that this is indeed the case. As a result, this process leads rather to thinning instabilities in the locally overheated FSSF than to thickening.

6 Dynamic characteristics of thickness instabilities

The aim of this section is to characterize the dynamics of thinning and thickening in FSSF. Both cases deal with nucleation and growth of dislocation loops, hence the physics behind these processes have much in common.

As discussed in sect. 4.4, the dynamics of the dislocation loops growth at thinning has been studied experimentally using a heating wire [10, 18–21]. For the liquid crystal 8CB the growth velocity of dislocation loops was found to be of the order of $v_{dl} \sim 10^{-6}\,\mathrm{m\,s^{-1}}$. Hereafter we show that our theoretical estimates are close to this value.

Regarding the thickening process, the question about characteristic times still remains open. From the experiments [15] we know that the time of growth of a thick island is of the order of a minute for several tens of layers, *i.e.* much faster than the thinning of overheated films (10^3 s, see sect. 4.4). As generation of elementary dislocation loops is the only way to change the number of layers in a FSSF (see appendix A and B), our numerical estimations should be based on dislocation loop dynamics.

In the following we use the general theoretical approach to study dislocation loop dynamics as proposed in refs. [10, 21]. It is based on the dissipation theorem and equates the energy gained by the FSSF and meniscus during loop growth to the total energy, dissipated in the system during this process:

$$\frac{\mathrm{d}W}{\mathrm{d}t} = -\Sigma, \tag{56}$$

where $\mathrm{d}W/\mathrm{d}t$ is the gain in total energy, eq. (2), per unit time due to loop growth, and Σ is the dissipated energy per unit time (neglecting inertial effects). The main contribution to the dissipated energy is due to friction: $\Sigma \approx 2\pi R G_x^{(\mathrm{fric})} v_x$, where $G_x^{(\mathrm{fric})}$ is the frictional force and v_x the velocity of the growing loop [10, 21].

The growth of a dislocation loop proceeds either by flow to the meniscus (thinning) or by supply of material from the meniscus (thickening). Furthermore, energy is dissipated by flow of material around the loop. The viscous friction sets certain restrictions to the velocity of loop growth, v_x, which determines the corresponding component of viscous stress tensor: $\sigma'_{xz} = \eta \partial v_x / \partial z$. According

to ref. [59] the friction force can be estimated as

$$G_x^{(\mathrm{fric})} \sim \int \sigma'_{xz} \mathrm{d}x \sim \eta\, v_x\, \delta_p\, \frac{1}{\sqrt{\lambda_p\, \eta}}\,, \tag{57}$$

where η is a viscosity for molecular motion perpendicular to the layers; λ_p the so-called permeation constant, and δ_p a length characterizing the permeation. For $T > T_{\mathrm{NA}}$ $\delta_p \backsimeq \xi$, in smectic phase $\delta_p \backsimeq 10^{-9}\,\mathrm{m}$ [16,59].

After differentiation of eqs. (31) or (53), the minimal work necessary for creation of a loop of radius R, with respect to t, and substitution of the result into eq. (56) we find

$$-\frac{1}{2\pi R}\frac{\partial W}{\partial R} v_x = G_x^{(\mathrm{fric})} v_x, \tag{58}$$

where $\partial W/\partial R$ is given by

$$-\frac{1}{2\pi R}\frac{\partial W}{\partial R} \approx -\Delta f - \frac{E_d}{R}\,. \tag{59}$$

Equation (59) has a simple interpretation in terms of effective forces acting on a dislocation loop. The first term on the right is the driving thermodynamic force for dislocation loop growth that can be identified as a Peach-Koehler force $G_x^{(\mathrm{PK})}$. The second term is due to variation in the line energy of the dislocation that represents the inward line tension force $G_x^{(t)}$ and opposes the extension of the loop (compare ref. [21]).

According to eqs. (57) and (58), the velocity of loop growth v_x is proportional to $\partial W/\partial R$. This relation is quite general and follows from the dynamical theory of growth of the critical nucleus [76]. The velocity of the dislocation loop growth v_x is determined from the balance of the overall driving force $G_{st} = G_x^{(\mathrm{PK})} + G_x^{(t)}$ and the friction force

$$G_{st} = G_x^{(\mathrm{fric})}. \tag{60}$$

Finally we obtain for v_x

$$v_x \sim G_{st} \frac{\sqrt{\lambda_p\, \eta}}{\eta\, \delta_p}\,. \tag{61}$$

Now we are ready to make an estimate of v_x using eqs. (57)–(61) and FSSF parameters. First, we consider the dynamics of thinning in an overheated smectic films. Taking liquid crystal parameter values from table 1, we obtain as value of the dislocation loop growth $v_x \sim 4 \cdot 10^{-6}\,\mathrm{m\,s^{-1}}$ (5O.6). For the compound 8CB the result is $v_x \sim 0.6 \cdot 10^{-6}\,\mathrm{m\,s^{-1}}$. Both values are in good agreement with the measured velocity of dislocation loop growth $v_{dl} \sim 10^{-6}\,\mathrm{m\,s^{-1}}$ from [19,21].

Now, let us estimate the velocity of dislocation loop growth for film thickening. For nucleation of the first dislocation loop of an excess smectic layer the overall driving force reaches the value $G_{st} \sim 2 \cdot 10^{-5}\,\mathrm{N\,m^{-1}}$. This is an order of magnitude larger than the value for thinning, due to the larger energy gain. Furthermore, the permeation length δ_p is an order of magnitude smaller. As a result, for thickening the velocity of loop growth is two orders of magnitude larger than for thinning transitions: $v_x \sim 0.5 \cdot 10^{-3}\,\mathrm{m\,s^{-1}}$. The value of v_x is large enough for material from the meniscus to fill up the vacant space at the footprint (size of a few mm) in a matter of seconds. Thus the film under the heated area grows layer by layer, forming a thick island in the film.

7 Concluding remarks

We have studied theoretically different thickness instabilities that occur in free-standing smectic films (FSSF) upon changing the external conditions. First, we explained the origin of thinning transitions in FSSF heated above their bulk smectic-nematic (isotropic) transition. According to our findings, upon overheating an additional normal tensile force appears as result of thermal expansion. The free energy of the system turns out to have an oscillatory character, and the equilibrium value of the film thickness shifts continuously toward the upper limit of the corresponding allowed zone. At this point the balance of the tensile and elastic force breaks down spontaneously, leading to mechanical instability of the film. The balance can be restored upon spontaneous thinning of the film. Generally a regular series of such thinning transitions occurs, in which the excess layers spills over to the meniscus. This process necessary includes nucleation and growth of dislocation loops in the middle plane of the film.

We calculated the activation energy of such dislocation loops near the critical points where the balance of forces breaks down, and find that the probability of nucleation is high. We determined the thermodynamic conditions for a sequence of thinning transitions and derived expression for the envelope of the actual thinning transition points. The latter are determined by the activation energy and the probability of loop formation. Additionally we estimated the characteristic times of dislocation loop growth. The expressions for both the envelope of thinning points and the dynamics of dislocation loops growth are in good agreement with experiments.

We have provided an explanation for the effect of thickening of FSSF, which occurs within the thermal range of the bulk smectic phase. We showed that local heating of a smectic film by an evanescent X-ray beam causes additional stress, resulting in changes of the mean density of the medium. This leads to extra contributions in the free-energy density of the system, of which the most important one arises from local thermal expansion of the FSSF.

We showed that at relatively large heating (but not too large, to avoid any transition to the nematic or isotropic state) nucleation and growth of dislocation loops of excess smectic layers in the middle plain of the film becomes energetically favorable. At a certain stage of heating, the activation energy for the formation of such dislocation loops becomes smaller than the threshold energy and decreases upon further heating. This leads to thickening of the film by many tens of layers, in good accordance with experimental observations. The realization of this scenario crucially depends on the energy dissipated locally in the film. The velocity of the dislocation loop of excess layer growth was estimated to be about $0.5 \cdot 10^{-3}\,\mathrm{m\,s^{-1}}$. This fits well to experiments on a thin film for which the speed of growth

of the thick "island" in the footprint area was about a layer per second [15].

Contrary to thinning of overheated FSSF, for which a whole set of experiments has been made [5, 7, 20, 23–25, 30, 31], observations of thickening are quite rare [15, 32]. Actually, our theoretical work was guided primarily by the experiment of ref. [15], in which heating was locally provided by absorption of an evanescent X-ray wave. Further experimental studies of thickening in FSSF would be very welcome. These should include different sources and various conditions of heating and external pressure. In addition it would be valuable if the thickening process was monitored optically.

An interesting and self-sufficient problem is the behavior of the meniscus at heating above the temperature of the bulk smectic-nematic transition, $T = T_{\rm NA}$. According to experiments by Demikhov *et al.* [8], at this point the size of the meniscus diminishes considerably while material is leaking out of the frame. This can be attributed to the disappearance of edge dislocations which constitute the smectic meniscus, because the meniscus is now in the nematic phase. We anticipate that the sign of the curvature of the meniscus will change. As a result the contact angle between the meniscus and the flat part of the film will increase, as observed by Picano *et al.* [20]. Hence measurements of the meniscus profile at temperatures above $T_{\rm NA}$ (and similarly above $T_{\rm IA}$) would be of special interest.

The authors thank E.E. Gorodetskii and V.E. Podnek for fruitful discussions and participation in the initial stages of this project. Particular thanks are due to E.I. Kats for helpful comments on the manuscript. The work of E.S. Pikina and B.I. Ostrovskii is funded by Russian Science Foundation (Grant No. 14-12-00475).

Author contribution statement

All authors contributed equally to the paper.

Appendix A. Free energy and profile of the meniscus of a FSSF

Nucleation of dislocations in a FSSF has clear implications for the of meniscus by which the film is attached to the supporting frame (see fig. 1). Actually the height of the meniscus depends on the number of dislocations that move to the meniscus during the process of film formation [20]. The aim of this appendix is twofold. First, we derive the expression for the excess free energy of the meniscus, and then calculate the meniscus profile. The shape of the meniscus is crucial to validate any theory describing the stability of a FSSF. Here we make an attempt to justify our theoretical approach by calculation of the shape of the meniscus and comparing with profiles determined experimentally.

According to [19], dislocations in the meniscus are always so close to each other, that they cannot be considered as independent. The distance between two neighboring elementary dislocations is larger than the width of the distortion they produce at the free surfaces of the meniscus [19]. In this limit the dislocations can be replaced by a continuous distribution of infinitesimal dislocations along the radial r axis [19]. This regime extends from the point matching with the planar part of the film, $r = r_{fl}$, to $r = r_0$. The value of r_0 determines the distance over which the approximation of a continuous distribution of infinitesimal dislocations is valid $r_0 \lesssim R_0$, where R_0 is the radius of the frame. The radius r of the film is measured from the center of the film.

The free energy associated with the dislocations contains their self-energy as well as the interactions between the dislocations. The contribution from the self-energy can be written as [19, 20]

$$\Delta F_{\rm men}^{(\rm self)} \approx 2\int_{r_{fl}}^{r_0} E_d \frac{1}{\delta h_{st}} \frac{{\rm d}h_m}{{\rm d}r} 2\pi r \, {\rm d}r, \tag{A.1}$$

where we introduced $h_m = h/2$ and $\delta h_{st}^{-1}({\rm d}h_m/{\rm d}r)$ is the local density of the dislocations. Upon writing the contribution to the dislocation energy of the meniscus proportional to the line energy, E_d, we actually take the excess surface energy into consideration (proportional to the surface tension γ), which is related to the presence of dislocations in the middle plane of the film (see eqs. (33), (35)). The height of the meniscus changes due to variation inside the meniscus of the number of dislocations from the planar part of the film. Accordingly, when we add the self-energy to the free energy of the meniscus, proportional to E_d, we implicitly assume that the inclination of the meniscus is caused solely by dislocations. This means that we do not include in the free energy of the meniscus a surface term of the type $2\gamma\int 2\pi r\,{\rm d}r\sqrt{1+(\partial h_m/\partial r)^2}$ as is often done (see, for example, [19]) because the main excess surface free energy has been included already in the self-energy of each dislocation.

There are two contributions to the dislocation interactions. The first has an entropic origin, while another is elastic and related to the strain fields [69, 70, 77]. As shown in [69] for a meniscus with a height smaller than $6\cdot10^{-5}$ m the elastic contribution to the interaction can be neglected relative to the entropic one. Thus the dominant force between steps at the free surfaces is due to entropic repulsion.

Entropic interactions between neighboring dislocations lead to an additional repulsive part in the free energy of the meniscus [77]. Thermal fluctuations of steps at the free surface of the meniscus caused by dislocations are limited in space by their neighbors. That causes to a loss of entropy and thus increases the free energy of the meniscus. In analogy to refs. [77, 78] it can be shown that the entropic repulsion energy between two neighboring steps on the free surface of the meniscus is of the order $\Phi\Delta x^{-2} \approx \Phi(\delta h_{st})^{-2}({\rm d}h_m/{\rm d}r)^2$ per unit length, with amplitude $\Phi \approx (k_BT/\pi)^2(E_{st})^{-1}$; Δx is the distance between neighboring steps of height δh_{st}.

The contribution of the entropic repulsion to the free energy of the meniscus is (see, for example, ref. [77]):

$$\Delta F_{\rm men}^{\rm (int)} \approx 2\int_{r_{fl}}^{r_0} \frac{\Phi}{\delta h_{st}^3}\left(\frac{{\rm d}h_m}{{\rm d}r}\right)^3 2\pi r\,{\rm d}r. \tag{A.2}$$

It is instructive to include also the contribution from gravitation

$$\Delta F_{\rm men}^{\rm (grav)} \approx \int_{r_{fl}}^{r_0} \frac{\varrho\, g (2h_m)^2}{2} 2\,\pi\, r\,{\rm d}r, \tag{A.3}$$

that in certain cases the role of gravity cannot be disregarded.

We have made several simplifications in the above integrals. Because the size of the frame is much larger than the lateral size of the meniscus, we replaced in the integrals the multiplier r by a constant r_0. The contribution from the free energy of the meniscus $\Delta F_{\rm men}$ can then be written as

$$\Delta F_{\rm men} = 2\,\pi\, r_0 \int_{r_{fl}}^{r_0} f[\vartheta, 2h_m[r]]{\rm d}r. \tag{A.4}$$

Taking together all contributions from above, the total energy of the meniscus becomes:

$$F_{\rm men}^{\rm (tot)} = \Delta F_{\rm men} + 2\,\pi\, r_0 \int_{r_{fl}}^{r_0} {\rm d}r \left[\frac{\varrho\, g (2\,h_m)^2}{2} + 2\left\{\frac{\Phi}{\delta h_{st}^3}\left(\frac{{\rm d}h_m}{{\rm d}r}\right)^3 + E_d \frac{1}{\delta h_{st}}\frac{{\rm d}h_m}{{\rm d}r}\right\}\right]. \tag{A.5}$$

This free energy of the meniscus can be naturally incorporated into the general expression for the total energy of the system, eq. (2), by adding of the energy contributions from the flat part of the film.

We now turn to the derivation of the meniscus profile. To the best of our knowledge there are two precise experiments to measure the shape of the meniscus [18,20]. Both were made at temperatures in the range of bulk smectic order and at atmospheric pressure. The profile of the meniscus was determined by observing the interference fringes in monochromatic light. We assume that the Burgers vector of each dislocation is equal to the layer thickness d_0, and that the total number of dislocations is fixed and given by $2h_0/d_0$, where h_0 is the height of the meniscus at the wall [52].

We take into account that for the geometry used ${\rm d}h_m/{\rm d}r > 0$. By varying $F_{\rm men}^{\rm (tot)}$ eq. (A.5) with respect to $h_m[r]$ we determine the conditions of equilibrium of the meniscus incorporating also the external pressure $p_{\rm air}$

$$3\frac{\Phi}{\delta h_{st}^3}\frac{\rm d}{{\rm d}r}\left\{\left(\frac{{\rm d}h_m}{{\rm d}r}\right)^2\right\} = 2\,\varrho\, g\, h_m + \big(({\rm d}f/{\rm d}h_m) + p_{\rm air}\big). \tag{A.6}$$

This equation can be solved using successive-approximations method. The terms in the second part on the right are several orders of magnitude larger than the other ones. Thus in the zeroth-order approximation we have

$$\frac{{\rm d}f}{{\rm d}h_m} + p_{\rm air} = 0. \tag{A.7}$$

This equation is similar to the condition for the balance of forces acting on the free surfaces of the flat part of FSSF (compare eqs. (48) and (50)) and defines the magnitude of the deformation of the layers, eq. (51).

Introducing eq. (A.7) into eq. (A.6) we can write the following equation:

$$3\frac{\Phi}{\delta h_{st}^3}\frac{\rm d}{{\rm d}r}\left\{\left(\frac{{\rm d}h_m}{{\rm d}r}\right)^2\right\} = 2\,\varrho\, g\, h_m. \tag{A.8}$$

The solution of of this equation gives us the desired dependence of $h_m(r)$. This procedure is analogous to the one presented in ref. [19], where the profile of meniscus was calculated under the assumption $\Delta p = 0$.

We can find an approximate analytical solution of eq. (A.8) by substituting $({\rm d}h/{\rm d}r) = \tan\theta$, where θ is the angle of inclination of the tangent to $h(r)$. Then eq. (A.8) can be rewritten in the form

$$\frac{\rm d}{{\rm d}r}\left\{(\tan\theta)^2\right\} = \frac{2\varrho g}{3\varkappa}\int \tan\theta\,{\rm d}r, \tag{A.9}$$

where

$$\varkappa = \frac{\Phi}{\delta h_{st}^3}. \tag{A.10}$$

To find an approximate solution of eq. (A.9) we neglect the h_m dependence of the parameter E_{st} in $\varkappa$ as more slow in comparison with ${\rm d}h_m/{\rm d}r$.

As boundary conditions we choose: $h[r_{fl}] = h_{fl}$, $({\rm d}h/{\rm d}r)_{r_{fl}} = \tan[\theta_f]$, $\tan\theta \approx \theta$, because $\tan\theta \ll 1$. Due to the subtle fall off of $\theta[r]$, we can neglect the dependence of θ on r, and make the integration in eq. (A.9). After some elementary calculations we arrive at

$$\frac{\rm d}{{\rm d}r}\{\theta^2\} = \frac{2\,\varrho\, g}{3\varkappa}\theta\, r + C_1. \tag{A.11}$$

Now the solution of eq. (A.11) for given boundary conditions can be obtained in the form

$$h_m[r] = \frac{\varrho g}{9\varkappa}(r - r_{fl})^3 + \theta_f(r - r_{fl}) + h_{fl}. \tag{A.12}$$

In order to make a direct comparison with the experiment of Picano *et al.* [20] we use the following numerical parameters: $r_{fl} = R_0 - X = 2.417\cdot 10^{-3}$ m, where R_0 is the radius of the frame, $R_0 = 2.5\cdot 10^{-3}$ m; X is the distance from the frame edge to the point of the meniscus meets the flat part of the film, $X = 83.125\cdot 10^{-6}$ m; $\theta_f \approx 0.009\pi$ and $h_{fl} = 5.51\cdot 10^{-8}$ m and the parameters of 8CB from table 1. Estimating $\delta h_{st} \sim d_0/2$ and $E_{st} \simeq 4\cdot 10^{-13}\,{\rm J\,m^{-1}}$ we get $\varkappa \sim 1.1\cdot 10^{-3}$. Finally, we obtain the solution of eq. (A.11) given by (A.12), which is shown in fig. 9. In the same figure the experimental meniscus profile from the ref. [20] is displayed. The profile calculated here on the basis of

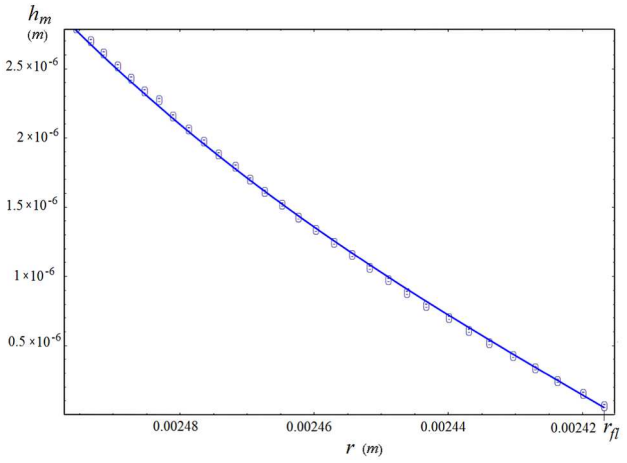

Fig. 9. Analytical profile $h_m(r)$ (by eq. (A.12)) and the profile of the meniscus from [20], elongated symbols indicate the experimental error.

eq. (A.6) is close to the experimental one from ref. [20], where the profile was approximated by a circular shape.

Thus, we have shown that the combination of entropic repulsion and gravitational terms in the total energy of the meniscus, is sufficient to derive a meniscus profile that agrees with experiment. This confirms the validity of our approach to describe thickness instabilities in FSSF.

Finally we note that the meniscus profile of the overheated FSSF can be different from that in a regular FSSF. In particular, at temperatures above the bulk $T_{\rm NA}$ ($T_{\rm IA}$), to secure the film stability the meniscus curvature can change sign. This question requires separate theoretical and experimental consideration.

Appendix B. Stretching of free-standing smectic films

In this appendix we address the rather complex process of fabrication of a FSSF of homogeneous thickness. As mentioned in sect. 2, FSSF can be drawn by moving a spreader across the opening in a glass or metal holder, while the edges have been wet with smectic material. During this process a number of dislocations loops are formed in the film and move to the meniscus. As a result the thinner regions grow at the expense of the thicker ones and the film becomes homogeneous.

To spread the film we attach a certain stress $\sigma_{xx}^{(0)}$ to the moving part of the device (x is a coordinate in the plane of the film along the stretching direction). The above force works to increase the surface area of the film, while also changing the mean density.

The relevant free energy of the system is given by eq. (7). As the film is stretched at constant temperature, all terms dependent on ΔT vanish. We first calculate the variation of the free energy of eq. (7) with ϑ and subsequently equate the resulting expression to $\sigma_{xx}^{(0)}$. Thus we arrive at the equilibrium condition of the system (along x)

$$A\vartheta - C\frac{[\phi]_N}{q_0 h} = -\sigma_{xx}^{(0)}. \tag{B.1}$$

The second term in this equation is much smaller than the first one (as we discussed above $q_0 h \gg [\phi]_N$ and $C \ll A$ (see p. 10)). Accordingly we obtain

$$\vartheta \approx -\frac{\sigma_{xx}^{(0)}}{A}, \tag{B.2}$$

where $\vartheta = \delta\rho/\rho_0$ equals the $-\delta l_x/l_0$, that is taking with the opposite sign relative displacement along the x axis under action the of the external force. Note that eq. (B.2) actually describes a small density variation related to a small adiabatic change of pressure (see, for example, ref. [33]).

We consider the variation of the free energy, eq. (7), over h, where $f_{Sm}[h]$ is represented by eq. (46). Taking into account that $\mathrm{d}f_{Sm}^{(T<T_{\rm NA})}[h]/\mathrm{d}h \approx B_b[\Delta u]_N/h$ and $[\phi]_N/(q_0 h) = [\Delta u]_N/h$, the condition of balance of the normal stresses can be written as

$$\eta \equiv \eta_N = \frac{[\Delta u]_N}{h} = \frac{1}{B_b}\left[C\,\vartheta - \frac{A}{2}\vartheta^2\right]$$
$$-\frac{B_b}{8(q_0\,\xi)^2} = -\frac{\sigma_{xx}^{(0)}}{A}\left[\frac{C}{B_b} + \frac{\sigma_{xx}^{(0)}}{2\,B_b}\right]. \tag{B.3}$$

Hence stretching applied in the plane of film leads to compression due to the negative sign on the right-hand part of eq. (B.3). This means for the smectic layer structure that stretching induces stress in the direction of the layer normal, $\sigma_{zz} \simeq B_b \partial u/\partial z = B_b \eta_N$.

Remarkably FSSF have a planar central part adjusted to a meniscus (we do not consider here thermally excited layer undulations in the films [9]). This distinguishes them from curved films of ordinary fluids. Initially moving the spreader across the edges of the frame produces some nonuniformity in the thickness. More importantly, the stretching force by itself produces dislocation loops in the middle plane of the film. This can be understood as follows.

Initially, the planar area of the stretched film is compressed. However, a further increase of the volume of the compressed film is energetically unfavorable and the system prefers to thin via formation of a dislocation loop of the missing layer. Taking eq. (B.3) into account, the work of formation of a dislocation loop in the middle plane of the FSSF can be written as

$$W_d = E_d 2\pi R - B_b \eta^2 d_0 \pi R^2. \tag{B.4}$$

The first term is the excess line energy of an elementary dislocation inside the FSSF (including both bulk and surface contributions as discussed in sect. 4.2). The second term is the free-energy gain of the system at thinning by one layer, d_0, which diminishes the elastic energy of the film due to a decreased number of stressed

layers. Accordingly, the work necessary to create a dislocation loop of critical radius reads: $W_c = \pi E_d R_c$, where $R_c = E_d(B_b\eta^2 d_0)^{-1}$. In order to create such a loop, the work of the external force $W_\sigma \sim \pi\sigma_{xx}^{(0)}\delta l_x d_0 R_c$ (at the displacement δl_x along the x axis) should exceed the barrier energy W_c. Taking into account that $\delta l_x \approx -\vartheta l_x^{(0)}$ (see comment after (B.2)), we obtain the following threshold condition for $\sigma_{xx}^{(0)}$

$$\sigma_{xx}^{(0)} > \left\{\frac{E_d A}{l_x^{(0)} d_0}\right\}^{\frac{1}{2}}. \tag{B.5}$$

Estimating $l_x^{(0)} \sim 10^{-3}\,\mathrm{m}$ and for the upper limit for E_d: $E_d \sim 10^{-12}\,\mathrm{J\,m^{-1}}$, we obtain $\sigma_{xx}^{(0)} > 3\cdot 10^4\,\mathrm{N\,m^{-2}}$. Taking for the surface of the spreader about $\sim 10^{-6}\,\mathrm{m^{-2}}$ we arrive at a rather low threshold force of 0.03 N (that is of the order of the weight of 3 g water).

In conclusion, the stretching stress, $\sigma_{xx}^{(0)}$, produces dislocation loops of missing smectic layers inside the FSSF. The normal component of stress, σ_{zz}, in turn exerts a Peach-Koehler force

$$\mathbf{G}^{(\mathrm{PK})} = (\sigma_{zz}\cdot\mathbf{b})\times\mathbf{t}, \tag{B.6}$$

with magnitude $\sigma_{zz}d_0$ acting on dislocations of Burgers vector d_0 in the plane of the film ($\mathbf{t}$ is the unit tangent to the dislocation line). This force cause the dislocation loops to move to the meniscus. Once the stretching force is released, the film equilibrates (slowly) to a uniform thickness. The combined action of stretching and compression stresses tends to make the film thinner, opening the possibility to create FSSF of homogeneous thickness.

Obviously, fabrication of a FSSF is an irreversible thermodynamic process because nucleation of dislocations is involved. This can be contrasted with ordinary liquids for which the final state of a film is governed by competition between surface tension and gravity, and will be always the same. For FSSF variations in stretching lead to different final states depending on the number of dislocation loops generated.

Appendix C. Calculations of the temperature changes during the thickening process

In this section we calculate the temperature changes in the film volume under footprint. The specific heating conditions during thickening of FSSF under absorption of the evanescent X-ray wave were as follows [15]. The FSSF was irradiated by X-rays below the critical angle for total reflection $\alpha < \alpha_C$ (see sect. 2). The experiments were made on 3 to 80 layer films of the liquid crystal compound 4O.8. In all cases the film thickened by many tens of layers along the beam footprint. We consider the thickening effect as discrete process in which successive excess smectic layers are generated. It is convenient to describe the continuous heating of the film as occurring at discrete time scale with periodicity δt.

In the following we consider the thickening of a FSSF of 4O.8 of initially four layers studied in [15]. The film was drawn over the opening in the frame of diameter $5\cdot 10^{-2}$ m. We define the perimeter of the beam footprint as $\Lambda_{fp} = 4.4\cdot 10^{-2}\,\mathrm{m}$, the square of the footprint $S_{fp} = 4\cdot 10^{-5}\,\mathrm{m^2}$, and the volume of the film of the thickness h under the footprint as $V_{fp} = hS_{fp}$, with $V_{fp}^{(0)} = 4.576\cdot 10^{-13}\,\mathrm{m^3}$. The initial temperature of the cold film is $T_0 = T_{\mathrm{NA}} - 13.5\,\mathrm{K}$. From the experiment [15] we know that during one second ($\delta t = 1\,\mathrm{s}$) the heat release constitute

$$Q = P\delta t \approx 2.8\cdot 10^{-6} J. \tag{C.1}$$

This leads to an increase of the initial temperature in the top two layers of the film under footprint of the order of $Q(c_p\rho_0 V_{fp}^{(0)}/2)^{-1} = 6.12\,\mathrm{K}$ ($c_p \approx 2\cdot 10^3\,\mathrm{J/(kg\ K)}$ is a specific heat). Taking into account that heat diffusivity in liquid crystals is $D_{H,L} \sim 10^{-7}\,\mathrm{m^2\,s^{-1}}$ [79,80], this means that all four layers in the film under the footprint heat up in $(2d_0)^2/D_{H,L} \sim 0.4\cdot 10^{-9}\,\mathrm{s}$, that is extremely fast. As a result in first time interval of 1 second the full volume under the footprint will be heated up by $\Delta T_{1\,0} = 3.06\,\mathrm{K}$ relative the cold part of the film.

The size of the film in the lateral direction is much larger, about 10^{-2} m. As a result, temperature equilibrium in this direction will be relatively slow: during a minute of irradiation the heat diffuses for about $2.45\cdot 10^{-3}$ m, which is an order of magnitude smaller than the lateral size of the film. These estimates indicate that the meniscus will not be heated yet and that any mass flow from the meniscus occurs at the initial temperature.

For the case of a four layer film it is convenient to divide the heating into intervals δt of one second because the growth of the excess smectic layers occurs at the same time scale. Furthermore, for the calculations we will use the following notations: ΔT_{ij} is the temperature change before j-thickening, (i is the number of the seconds counted from the beginning of the heating process, j is the number of the successive layer thickening); $\Delta T_{ij}^{(c)}$ is the diminished temperature change after nucleation of the dislocation loop of the excess smectic layer.

During heating of the film some energy from the film footprint volume diffuses into the surrounding space. For convenience the dissipation of heat arriving at the current time interval is considered from the next interval. The volume over which the heat diffuses during the time t can be estimated as $\sqrt{D_{H,L}t}\Lambda_{fp}h^{(0)} \approx 1.59\sqrt{t}\cdot 10^{-13}\,\mathrm{m^3}$. To simplify the calculations we neglect the heat diffusion through the air and assume that the heat conduction takes place only in the lateral direction along the footprint perimeter Λ_{fp} of the volume of height $h^{(0)}$, where direct contact with the cold part of the film occurs.

We find that the first dislocation loop of the critical radius in the middle plane of the film is generated only after the third second of heating. The corresponding expressions for temperature difference between the enhanced

footprint volume and the cold part of the film are:

$$\Delta T_{31} = \frac{Q}{c_p\rho_0}\Big\{V_{fp}^{(0)} + \sqrt{D_{H,L}(t_3-t_1)}\Lambda_{fp}h_0\Big\}^{-1} + \frac{Q}{c_p\rho_0}\Big\{V_{fp}^{(0)} + \sqrt{D_{H,L}(t_3-t_2)}\Lambda_{fp}h_0\Big\}^{-1} + \frac{Q}{c_p\rho_0}\frac{1}{V_{fp}^{(0)}}, \quad (C.2)$$

$$\Delta T_{31}^{(c)} = \frac{Q}{c_p\rho_0}\Big\{V_{fp}^{(0)} + \sqrt{D_{H,L}(t_3-t_1)}\Lambda_{fp}h_0 + \pi(R)^2 d_0\Big\}^{-1} + \frac{Q}{c_p\rho_0}\Big\{V_{fp}^{(0)} + \sqrt{D_{H,L}(t_3-t_2)}\Lambda_{fp}h_0 + \pi(R)^2 d_0\Big\}^{-1} + \frac{Q}{c_p\rho_0}\frac{1}{V_{fp}^{(0)} + \pi(R)^2 d_0}, \quad (C.3)$$

where the time intervals t_k ($k = 1$–3) are the number of seconds from the beginning of heating process till the k second, R is the current radius of the dislocation loop.

Then after the fourth second of heating we can calculate the temperature difference between the footprint volume and the surrounding film before and after nucleation of the next dislocation loop

$$\Delta T_{42} = \frac{Q}{c_p\rho_0}\Big\{V_{fp}^{(h_1)} + \sqrt{D_{H,L}(t_4-t_1)}\Lambda_{fp}h_0\Big\}^{-1} + \frac{Q}{c_p\rho_0}\Big\{V_{fp}^{(h_1)} + \sqrt{D_{H,L}(t_4-t_2)}\Lambda_{fp}h_0\Big\}^{-1} + \frac{Q}{c_p\rho_0}\Big\{V_{fp}^{(h_1)} + \sqrt{D_{H,L}(t_4-t_3)}\Lambda_{fp}h_0\Big\}^{-1} + \frac{Q}{c_p\rho_0}\frac{1}{V_{fp}^{(h_1)}}, \quad (C.4)$$

$$\Delta T_{42}^{(c)} = \frac{Q}{c_p\rho_0}\Big\{V_{fp}^{(h_1)} + \sqrt{D_{H,L}(t_4-t_1)}\Lambda_{fp}h_0 + \pi(R)^2 d_0\Big\}^{-1} + \frac{Q}{c_p\rho_0}\Big\{V_{fp}^{(h_1)} + \sqrt{D_{H,L}(t_4-t_2)}\Lambda_{fp}h_0 + \pi(R)^2 d_0\Big\}^{-1} + \frac{Q}{c_p\rho_0}\Big\{V_{fp}^{(h_1)} + \sqrt{D_{H,L}(t_4-t_3)}\Lambda_{fp}h_0 + \pi(R)^2 d_0\Big\}^{-1} + \frac{Q}{c_p\rho_0}\frac{1}{V_{fp}^{(h_1)} + \pi(R)^2 d_0}. \quad (C.5)$$

Summarizing the above regularities, we can present equations for ΔT_{ij} and $\Delta T_{ij}^{(c)}$ in the form

$$\Delta T_{ij} = \frac{Q}{c_p\rho_0}\Big\{V_{fp}^{(h_{j-1})} + \sqrt{D_{H,L}(t_i-t_1)}\Lambda_{fp}h_0\Big\}^{-1} + \frac{Q}{c_p\rho_0}\Big\{V_{fp}^{(h_{j-1})} + \sqrt{D_{H,L}(t_i-t_2)}\Lambda_{fp}h_0\Big\}^{-1} + \ldots + \frac{Q}{c_p\rho_0}\Big\{V_{fp}^{(h_{j-1})} + \sqrt{D_{H,L}(t_i-t_k)}\Lambda_{fp}h_0\Big\}^{-1} + \ldots + \frac{Q}{c_p\rho_0}\frac{1}{V_{fp}^{(h_{j-1})}}, \quad (C.6)$$

and

$$\Delta T_{ij}^{(c)} = \frac{Q}{c_p\rho_0}\Big\{V_{fp}^{(h_{j-1})} + \sqrt{D_{H,L}(t_i-t_1)}\Lambda_{fp}h_0 + \pi(R)^2 d_0\Big\}^{-1} + \frac{Q}{c_p\rho_0}\Big\{V_{fp}^{(h_{j-1})} + \sqrt{D_{H,L}(t_{ij}-t_2)}\Lambda_{fp}h_0 + \pi(R)^2 d_0\Big\}^{-1} + \ldots + \frac{Q}{c_p\rho_0}\Big\{V_{fp}^{(h_{j-1})} + \sqrt{D_{H,L}(t_i-t_k)}\Lambda_{fp}h_0 + \pi(R)^2 d_0\Big\}^{-1} + \ldots + \frac{Q}{c_p\rho_0}\frac{1}{V_{fp}^{(h_{j-1})} + \pi(R)^2 d_0}. \quad (C.7)$$

References

1. G. Friedel, Ann. Phys. (Paris) **18**, 273 (1922).
2. P.S. Pershan, *Structures of Liquid Crystal Phases*, World Scientific Lecture Notes in Physics **23** (World Scientific, Singapore, 1988).
3. P. Pieranski, L. Beliard, J.-Ph. Tournellec, X. Leoncini, C. Furtlehner, H. Dumoulin, E. Riou, B. Jouvin, J.-P. Fenerol, Ph. Palaric, J. Heuving, B. Cartier, I. Kraus, Physica A **194**, 364 (1993).
4. C. Bahr, Int. J. Mod. Phys. B **8**, 3051 (1994).
5. S. Stoebe, P. Mach, C.C. Huang, Phys. Rev. Lett. **73**, 1384 (1994).
6. S. Stoebe, C.C. Huang, Int. J. Mod. Phys. B **9**, 2285 (1995).
7. E.I. Demikhov, Mol. Cryst. Liq. Cryst. Sci. Technol., Sect. A **265**, 403 (1995).
8. E.I. Demikhov, V.K. Dolganov, K.P. Meletov, Phys. Rev. E **52**, R1285 (1995).
9. W.H. de Jeu, B.I. Ostrovskii, A.N. Shalaginov, Rev. Mod. Phys. **75**, 181 (2003).
10. P. Oswald, P. Pieranski, *Smectic and Columnar Liquid Crystals: Concepts and Physical Properties Illustrated by Experiments* (Taylor & Francis, Boca Raton, London, New York, 2006) p. 447.
11. C. Bohley, R. Stannarius, Soft Matter **4**, 683 (2008).
12. P.G. de Gennes, Langmuir **6**, 1448 (1990).
13. L.V. Mikheev, A.A. Chernov, Zh. Eksp. Teor. Fiz. **95**, 2026 (1989) and reference 31 therein.

14. E.E. Gorodetskii, E.S. Pikina, V.E. Podnek, JETP **88**, 35 (1999) (Zh. Eksp. Teor. Fiz. **115**, 61 (1999)).
15. W.H. de Jeu, A. Fera, B.I. Ostrovskii, Eur. Phys. J. E **15**, 61 (2004).
16. P.G. de Gennes, J. Prost, *Physics of Liquid Crystals* (Clarendon Press, Oxford, 1993).
17. C.Y. Young, R. Pindak, N.A. Clark, R.B. Meyer, Phys. Rev. Lett. **40**, 773 (1978).
18. J.C. Géminard, R. Hołyst, P. Oswald, Phys. Rev. Lett. **78**, 1924 (1997).
19. F. Picano, R. Hołyst, P. Oswald, Phys. Rev. E **62**, 3747 (2000).
20. F. Picano, P. Oswald, E. Kats, Phys. Rev. E **63**, 021705 (2001).
21. P. Oswald, F. Picano, F. Caillier, Phys. Rev. E **68**, 061701 (2003).
22. P.M. Johnson, P. Mach, E.D. Wedell, F. Lintgen, M. Neubert, C.C. Huang, Phys. Rev. E **55**, 4386 (1997).
23. S. Pankratz, P.M. Johnson, H.T. Nguyen, C.C. Huang, Phys. Rev. E **58**, R2721 (1998).
24. V.K. Dolganov, E.I. Demikhov, R. Fouret, C. Gors, Phys. Lett. A **220**, 242 (1996).
25. E.A.L. Mol, G.C.L. Wong, J.-M. Petit, F. Rieutord, W.H. de Jeu, Physica B **248**, 191 (1998).
26. L.V. Mirantsev, Liq. Cryst. **20**, 417 (1996).
27. Y. Martínez-Ratón, A.M. Somoza, L. Mederos, D.E. Sullivan, Phys. Rev. E **55**, 2030 (1997).
28. A.N. Shalaginov, D.E. Sullivan, Phys. Rev. E **63**, 031704 (2001).
29. D.E. Sullivan, A.N. Shalaginov, Phys. Rev. E **70**, 011707 (2004).
30. S. Pankratz, P.M. Johnson, R. Hołyst, C.C. Huang, Phys. Rev. E **60**, R2456 (1999).
31. S. Pankratz, P.M. Johnson, A. Paulson, C.C. Huang, Phys. Rev. E **61**, 6689 (2000).
32. F. Bougrioua, P. Cluzeau, P. Dolganov, G. Joly, H.T. Nguen, V. Dolganov, Phys. Rev. Lett. **95**, 027802 (2005).
33. L.D. Landau, E.M. Lifshitz, *Fluid Mechanics* (Butterworth-Heinemann, Oxford, 1987).
34. L.D. Landau, E.M. Lifshitz, *Theory of Elasticity* (Science, Moscow, 1987) §§ 40–46.
35. S.M. Stishov, S.N. Nefedov, A.N. Zisman, JETP Lett. **36**, 348 (1982).
36. S.N. Nefedov, A.N. Zisman, S.M. Stishov, Sov. Phys. JETP **59**, 71 (1984).
37. S. Kralj, T.J. Sluckin, Phys. Rev. E **50**, 2940 (1994).
38. M. Slavinec, S. Kralj, S. Žumer, T.J. Sluckin, Phys. Rev. E **63**, 031705 (2001).
39. Z. Kutnjak, S. Kralj, G. Lahajnar, S. Žumer, Phys. Rev. E **70**, 051703 (2004).
40. P. Oswald, L. Lejček, Eur. Phys. J. E **19**, 441 (2006).
41. P. Richetti, L. Moreau, P. Barois, P. Kékicheff, Phys. Rev. E **54**, 1749 (1996).
42. A.E. Lord, Phys. Rev. Lett. **29**, 1366 (1972).
43. L. Ricard, J. Prost, J. Phys. **42**, 861 (1981).
44. H. Li, M. Kardar, Phys. Rev. A **46**, 6490 (1992).
45. A. Ajdari, L. Peliti, J. Prost, Phys. Rev. Lett. **66**, 1481 (1991).
46. E.S. Pikina, JETP **109**, 885 (2009) (Zh. Eksp. Teor. Fiz. **136**, 1023 (2009)).
47. E.S. Pikina, Mol. Cryst. Liq. Cryst. **546**, 95/[1565] (2011).
48. E.S. Pikina, C. Rosenblatt, Eur. Phys. J. E **35**, 87 (2012).
49. M.R. Fisch, P.S. Pershan, L.B. Sorensen, Phys. Rev. A **29**, 2741 (1984).
50. R.J. Birgeneau, C.W. Garland, G.B. Kasting, B.M. Ocko, Phys. Rev. A **24**, 2624 (1981).
51. P.S. Pershan, J. Prost, J. Appl. Phys. **46**, 2343 (1975).
52. R. Hołyst, P. Oswald, Int. J. Mod. Phys. B **9**, 1515 (1995).
53. P.S. Pershan, J. Appl. Phys. **45**, 1590 (1974).
54. L. Lejček, P. Oswald, J. Phys. II **1**, 931 (1991).
55. M.S. Turner, M. Maaloum, D. Ausserré, J.-F. Joanny, M. Kunz, J. Phys. II **4**, 689 (1994).
56. R. Hołyst, Phys. Rev. Lett. **72**, 4097 (1994).
57. P.G. de Gennes, C.R. Acad. Sci. Paris B **275**, 549 (1972).
58. M. Kléman, C.E. Williams, J. Phys. (Paris) Lett. **35**, L49 (1974).
59. M. Kléman, O.D. Lavrentovich, *Soft Matter Physics: An Introduction* (Springer-Verlag, New York, 2003).
60. S. Kralj, T.J. Sluckin, Liquid crystals **18**, 887 (1995).
61. P. Mach, C.C. Huang, T. Stoebe, E.D. Wedell, T. Nguyen, W.H. de Jeu, F. Guittard, J. Nacri, R. Shashidar, N. Clark, I.M. Jiang, F.J. Kao, H. Lui, H. Nohira, Langmuir **14**, 4330 (1998).
62. D. Davidov, C.R. Safinya, M. Kaplan, S.S. Dana, R. Schaetzing, R.J. Birgeneau, J.D. Litster, Phys. Rev. B **19**, 1657 (1979).
63. J.S. Langer, M.E. Fisher, Phys. Rev. Lett. **19**, 560 (1967).
64. E.I. Demikhov, M. John, K. Krohn, Liq. Cryst. **23**, 443 (1997).
65. P. Cluzeau, V. Dolganov, P. Poulin, G. Joly, H.T. Nguyen, Mol. Cryst. Liq. Cryst. **364**, 381 (2001).
66. R. Najjar, Y. Galerne, Mol. Cryst. Liq. Cryst. **367**, 3263 (2001).
67. H. Schüuring, R. Stannarius, Langmuir **18**, 9735 (2002).
68. H. Schüring, R. Stannarius, Mol. Cryst. Liq. Cryst. **412**, 425/[2035] (2004).
69. L. Lejček, J. Bechhoefer, P. Oswald, J. Phys. II **2**, 1511 (1992).
70. J. Bechhoefer, L. Lejček, P. Oswald, J. Phys. II **2**, 27 (1992).
71. A.J. Jin, M. Veum, T. Stoebe, C.F. Chou, J.T. Ho, S.W. Hui, V. Surendranath, C.C. Huang, Phys. Rev. E **53**, 3639 (1996).
72. N.A. Clark, Phys. Rev. A **14**, 1551 (1976).
73. E.E. Gorodetskii, V.E. Podnek, *Book of Abstracts of the 11th International Liquid Crystal, MA-9 Conference* (Berkeley, California, 1986).
74. V.E. Podnek, Ph.D. Thesis (Moscow, 1987).
75. P.G. de Gennes, F. Brochard-Wyart, D. Quéré, *Capillarity and Wetting Phenomena: Drops, Bubbles, Pearls, Waves* (Springer-Verlag, New York, 2004).
76. E.M. Lifshitz, L.P. Pitaevskii, *Physical Kinetics* (Science, Moscow, 1979) pp. 503–516.
77. P. Noziéres, *Shape and growth of crystals*, in *Solids far from Equilibrium, Beg Rohu Lectures*, edited by C. Godreche (Cambridge University Press, 1992).
78. P. Noziéres, F. Gallet, J. Phys. **48**, 353 (1987).
79. W. Urbach, H. Hervet, F. Rondelez, Mol. Cryst. Liq. Cryst. **46**, 209 (1978).
80. W. Urbach, H. Hervet, F. Rondelez, J. Chem. Phys. **78**, 5113 (1983).